

Journal Pre-proofs

Platinum Ethylene Dimerization Catalysts: Diphosphine vs. Diimine Ancillary Ligand Effects

Suman Debnath, Sayanti Basu, Bradley M. Schmidt, Jeramie J. Adams, Navamoney Arulsamy, Dean M. Roddick

PII: S0277-5387(20)30118-2
DOI: <https://doi.org/10.1016/j.poly.2020.114461>
Reference: POLY 114461

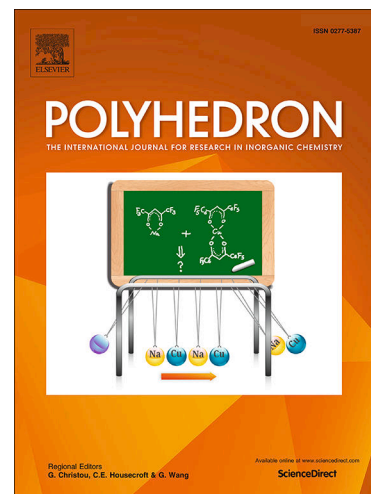
To appear in: *Polyhedron*

Received Date: 5 January 2020
Revised Date: 17 February 2020
Accepted Date: 17 February 2020

Please cite this article as: S. Debnath, S. Basu, B.M. Schmidt, J.J. Adams, N. Arulsamy, D.M. Roddick, Platinum Ethylene Dimerization Catalysts: Diphosphine vs. Diimine Ancillary Ligand Effects, *Polyhedron* (2020), doi: <https://doi.org/10.1016/j.poly.2020.114461>

This is a PDF file of an article that has undergone enhancements after acceptance, such as the addition of a cover page and metadata, and formatting for readability, but it is not yet the definitive version of record. This version will undergo additional copyediting, typesetting and review before it is published in its final form, but we are providing this version to give early visibility of the article. Please note that, during the production process, errors may be discovered which could affect the content, and all legal disclaimers that apply to the journal pertain.

© 2020 Published by Elsevier Ltd.



Revised

**Platinum Ethylene Dimerization Catalysts: Diphosphine vs.
Diimine Ancillary Ligand Effects**

Suman Debnath, Sayanti Basu, Bradley M. Schmidt, Jeramie J. Adams, Navamoney
Arulsamy, and Dean M. Roddick*

Department of Chemistry, University of Wyoming

Dept. 3838, 1000 E University Ave., Laramie, WY 82071

Abstract

Kinetic and mechanistic studies are presented for the previously reported (dfepe)Pt(Me)(NC₅F₅)⁺ (dfepe = (C₂F₅)₂PCH₂CH₂P(C₂F₅)₂) ethylene dimerization catalyst system. New labile complexes (dfepe)PtMe(L)⁺ (L = NC₅F₅, C₆F₅CN, C₆F₅NH₂, C₆F₅NO₂) have been prepared. A general extension to a variety of other chelating diphosphine analogues (PP)Pt(Me)(C₂H₄)⁺ has been accessed by methyl abstraction from donor (PP)PtMe₂ precursors with Ph₃C⁺B(C₆F₅)₄⁻ in the presence of ethylene to cleanly afford (PP)Pt(Me)(C₂H₄)⁺ products. Catalysis studies for these more electron-rich diphosphine systems demonstrate moderate dimerization activity which is uniformly higher than reported for (diimine)Pt(Me)(C₂H₄)⁺. In several cases allylic catalyst decomposition products (PP)Pt(η³-C₃H₄Me)⁺ have been identified. A DFT study of insertion barriers for diimine and diphosphine systems is presented which suggests that weakening of Pt-ethylene ground state binding by strong-field diphosphine ligands is a major contributing factor to the lower ethylene insertion barriers for PP systems.

[†]Submitted in honor of Prof. John E. Bercaw, on the occasion of his 75th birthday

Keywords (platinum organometallics; ethylene complex; phosphine coordination; DFT analysis; dimerization catalysis; kinetics)

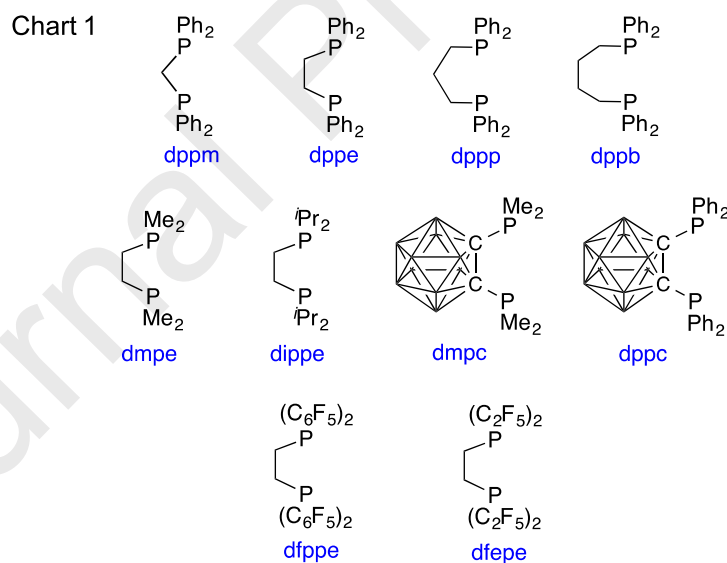
Introduction

Catalytic olefin oligomerization/polymerization continues to be a subject of considerable academic as well as industrial interest. Ziegler-Natta and chromium-based Phillips catalyst systems are well known and have been used for the past 60 years to facilitate olefin polymerization at low pressures and moderately high temperatures resulting in millions of tons of polyethylene and polypropylene each year.¹ Large scale linear alpha olefin production using the Shell higher olefin process is also well-established.² One major limitation of early-transition metal polymerization catalysts is their strong Lewis-acidic nature and oxophilicity, which makes them incompatible for use in polymerization or co-polymerization of many functionalized olefins. While late transition metal systems in principle are more tolerant of alkene functional groups because of their reduced affinities for heteroatoms (N, O, halides), late transition metal systems are still mostly limited to dimerization or oligomerization of simple alkenes.³

Pioneering work by Brookhart and coworkers in 1995 on highly active nickel (II) and palladium (II) α -diimine complexes has driven interest in late transition metal systems as efficient olefin oligomerization catalysts.^{4,5} In stark contrast, the analogous platinum diimine complex, (diimine)Pt(Et)(C₂H₄)⁺, was found to exhibit very limited ethylene dimerization activity (100 °C, ~ 0.1 turnovers hr⁻¹).⁶ The rate-limiting ethylene insertion barrier for platinum in this system was determined to be 29.8 kcal mol⁻¹, which is much higher than the corresponding barriers found for palladium (17-19 kcal mol⁻¹) and nickel (13-14 kcal mol⁻¹). In 1999 our research group reported modest ethylene dimerization activity for the perfluoroalkylphosphine (PFAP) system (dfep)Pt(Me)(O₂CCF₃) (80 °C, TOF = 6 hr⁻¹; dfep = (C₂F₅)₂PCH₂CH₂P(C₂F₅)₂).⁷ Noting that CF₃CO₂⁻ anion loss was likely the rate determining step, in 2008 we reported a labile platinum alkyl cation

$[(dfepe)Pt(Me)(NC_5F_5)]^+B(C_6F_5)_4^-$ which converts to the desired ethylene adduct $(dfepe)Pt(Me)(C_2H_4)^+$ upon exposure to ethylene at $-20\text{ }^\circ\text{C}$.⁸ $[(dfepe)Pt(Me)(NC_5F_5)]^+B(C_6F_5)_4^-$ is an active ethylene dimerization pre-catalyst at ambient temperature (600 psi ethylene, $27\text{ }^\circ\text{C}$ in *o*-difluorobenzene (DFB), TOF = 42 hr^{-1}).⁹ This activity is *many orders of magnitude greater* than the corresponding diimine catalyst and provided motivation for the further development of PFAP-based group 10 alkene oligomerization catalysts.

In this paper, we have examined the properties and dimerization kinetics of the $(dfepe)Pt(Me)(C_2H_4)^+$ catalyst in more detail, and also surveyed the ethylene dimerization activity for a range of chelating donor phosphine complexes $(PP)Pt(Me)(C_2H_4)^+$ with varying chelate backbones and pendant phosphine groups (Chart 1).



While the electron-poor PFAP complex $(dfepe)PtMe_2$ reacts only slowly with trityl cation, more electron-rich $(PP)PtMe_2$ complexes react readily with $Ph_3C^+B(C_6F_5)_4^-$ in the presence of ethylene to cleanly afford $(PP)Pt(Me)(C_2H_4)^+$ products. Ethylene dimerization activity of the donor phosphine systems was found to be significantly less than

(dfepe)Pt(Et)(C₂H₄)⁺, but still considerably more active than the platinum diimine system. DFT calculations are presented which provide some insight into the generally higher catalytic activity of group 10 phosphine-supported catalysts.

Results and Discussion

(dfepe)Pt(Me)(L)⁺ Chemistry

a) (dfepe)PtMe(L)⁺ (L = NC₅F₅, C₆F₅CN, C₆F₅NH₂, C₆F₅NO₂) Synthesis. We have briefly examined pentafluorobenzonitrile, pentafluoroaniline, and pentafluoronitrobenzene as alternative labile ligands for (dfepe)PtMe(L)⁺ chemistry. [(dfepe)PtMe(NC₅F₅)]⁺B(C₆F₅)₄⁻ (**1**) is only slightly soluble in pentafluorobenzonitrile at ambient temperature, but warming to 80 °C for 30 mins followed by cooling produced crystals of [(dfepe)Pt(Me)(C₆F₅CN)]⁺B(C₆F₅)₄⁻ (**2**) suitable for X-ray diffraction (Figure 1) which confirmed conversion to the pentafluorobenzonitrile adduct (Equation 1).

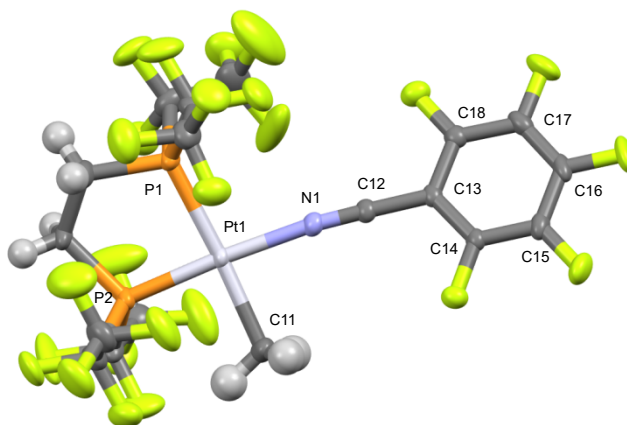
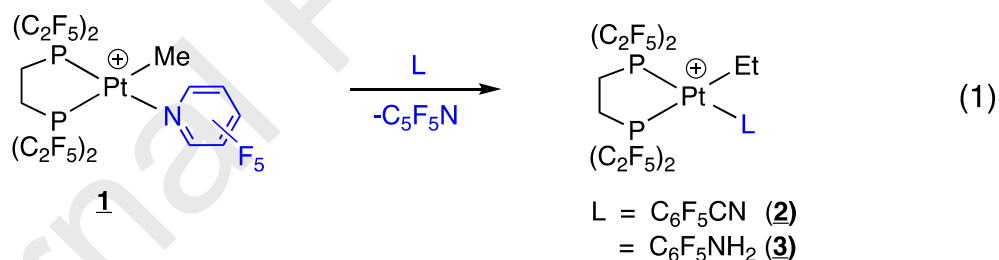
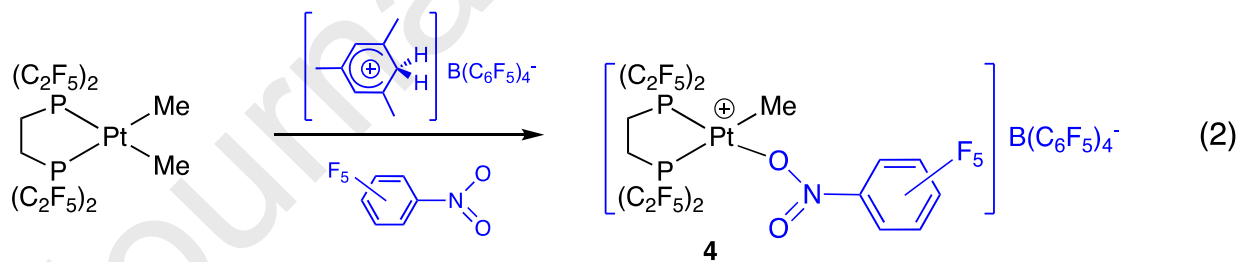


Figure 1. Molecular plot of [(dfepe)Pt(Me)(NCC₆F₅)]⁺B(C₆F₅)₄⁻ (**2**) (borate anion not shown) showing 50% probability thermal ellipsoids and partial labeling scheme. Selected metrical data (bond lengths in Å and angles in deg): Pt(1)-N(1): 2.044(3); Pt(1)-C(11): 2.104(3); N(1)-C(12): 1.133(4); Pt(1)-P(1): 2.2974(8); Pt(1)-P(2): 2.1736(9); P(1)-Pt(1)-N(1): 97.42(8); P(1)-Pt(1)-C(11): 175.2(1). P(2)-Pt(1)-N(1): 176.06(8), P(2)-Pt(1)-C(11): 91.16(12).

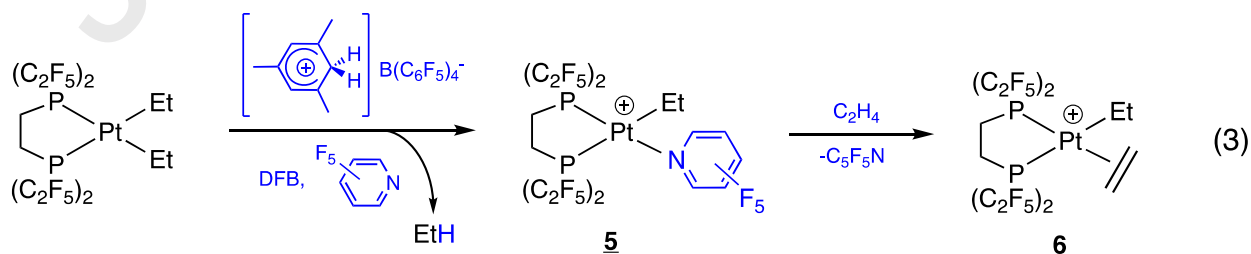
Reaction of **1** with 3 equiv. pentafluoroaniline in *o*-difluorobenzene at room temperature similarly resulted in the displacement of the pentafluoropyridine ligand to yield [(dfepe)Pt(Me)(NH₂C₆F₅)]⁺B(C₆F₅)₄⁻ (**3**). Adducts **2** and **3** were not isolated on a preparative scale. Pentafluoronitrobenzene was also examined as both a potential weakly-coordinating solvent and a useful ancillary ligand. No displacement of pentafluoropyridine was indicated by NMR spectra of **1** dissolved in pentafluoronitrobenzene; however, protonolysis of (dfepe)PtMe₂ with [H(mesitylene)]⁺B(C₆F₅)₄⁻ in pentafluoronitrobenzene as the solvent cleanly yielded a pale green product [(dfepe)Pt(Me)(C₆F₅NO₂)]⁺B(C₆F₅)₄⁻ (**4**), which was isolated in 76% yield (Equation 2).



For (dfepe)PtMe(L)⁺ complexes the relative ordering of ¹J_{PtP} magnitudes (*trans* to L) is: 5480 Hz (C₆F₅NO₂) >> 4950 (NC₅F₅) ~ 4940 (C₆F₅CN) >> 4450 (C₆F₅NH₂) > 4370 (C₂H₄)⁸, which parallels the qualitative ligand lability trend. While several platinum adducts of pentafluoroaniline and pentafluorobenzonitrile have been reported,^{10,11} to our

knowledge complex **4** is the only reported example of an isolated pentafluoronitrobenzene adduct.

b) (dfepe)PtEt(L)⁺ Synthesis and Dynamics. In our initial report we noted that (dfepe)PtMe(C₂H₄)⁺ cleanly formed upon treatment of the labile pentafluoropyridine adduct [(dfepe)Pt(Me)(NC₅F₅)⁺B(C₆F₅)₄⁻] with ethylene at -20 °C (³¹P NMR: δ 75.7 (¹J_{PtP} = 1360 Hz), 64.6 (¹J_{PtP} = 4370 Hz)).⁸ Monitoring the course of reaction by ³¹P NMR showed conversion to a catalyst resting state with similar spectroscopic features (-20 °C: δ 74.6 (¹J_{PtP} = 1220 Hz), 63.6 (¹J_{PtP} = 4730 Hz)), which we had tentatively assigned as the ethyl complex (dfepe)Pt(Et)(C₂H₄)⁺. We have now confirmed this assignment: protonolysis of (dfepe)PtEt₂ by [H(mesitylene)]⁺B(C₆F₅)₄⁻ in pentafluoropyridine cleanly generates [(dfepe)Pt(Et)(NC₅F₅)⁺B(C₆F₅)₄⁻] (**5**) which was isolated as a white solid containing 0.79 equiv. of unassociated pentafluoropyridine. Addition of excess (~ 5 equiv.) ethylene to **5** in DFB at -30 °C resulted in complete displacement of pentafluoropyridine within minutes to generate a product with ³¹P resonances essentially identical to those previously ascribed to (dfepe)Pt(Et)(η²-C₂H₄)⁺ (**6**) (Equation 3, Figure 2). Under excess ethylene ¹H NMR spectra show a single broadened ethylene resonance at 4.3 ppm due to rapid exchange. Exposure of **5** to a limiting (~10%) amount of ethylene resulted in partial conversion to **6** and the appearance of a ¹⁹⁵Pt-coupled C₂H₄ resonance at δ 4.76 (²J_{PtH} = 55 Hz).



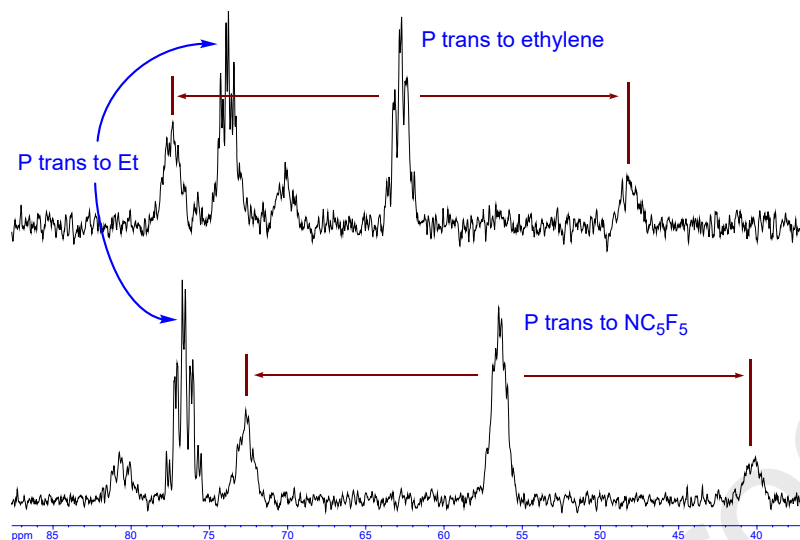


Figure 2. Bottom: ^{31}P NMR spectrum of $\{(\text{dfepe})\text{Pt}(\text{Et})(\text{NC}_5\text{F}_5)^+\}\text{B}(\text{C}_5\text{F}_6)_4^-$ in DFB at -30 °C. Top: treatment with excess ethylene at -30 °C, 30 min., conversion to $[(\text{dfepe})\text{Pt}(\text{Et})(\text{C}_2\text{H}_4)]^+\text{B}(\text{C}_5\text{F}_6)_4^-$.

The pentafluoropyridine adduct $(\text{dfepe})\text{Pt}(\text{Et})(\text{NC}_5\text{F}_5)^+$ displays dynamic NMR behavior. Ambient temperature spectra for $(\text{dfepe})\text{Pt}(\text{Et})(\text{NC}_5\text{F}_5)^+$ in *o*-difluorobenzene exhibit a single broad resonance at 0.4 ppm for all five ethyl protons. A coalescence point is reached at 0 °C and further cooling to -50 °C results in separate methylene and methyl resonances at δ 1.01 and -0.29 , respectively (Supplemental Figure S10). A slow exchange limit with fully resolved $^3J_{\text{HH}}$ splitting was not accessible due to the freezing point limit of the solvent (-34 °C). Coordinated pentafluoropyridine resonances for $(\text{dfepe})\text{Pt}(\text{Et})(\text{NC}_5\text{F}_5)^+$ are not observed in ambient temperature ^{19}F NMR spectra due to rapid ligand exchange with free residual pentafluoropyridine, but cooling to -50 °C revealed both free and coordinated $\text{C}_5\text{F}_5\text{N}$ resonances (Supplemental Figure S12). Line shape analysis for both Pt-ethyl proton exchange and NC_5F_5 ligand exchange (Figures S11, S13) give intra- and intermolecular kinetic barriers of $12.6(2)$ kcal mol $^{-1}$ and $11.8(2)$

kcal mol⁻¹, respectively, which are consistent with an ethyl site exchange mechanism involving initial NC₅F₅ ligand loss followed by reversible β-H elimination.

Dynamic exchange processes for (dfepe)Pt(Et)(η²-C₂H₄)⁺ could not be evaluated due to the onset of ethylene insertion chemistry above -30 °C.¹² Formation of (dfepe)Pt(Et)(η²-C₂H₄)⁺ followed by removal of excess ethylene led to uncharacterized product mixtures and no evidence of platinum hydride formation. Since treatment of (diimine)PtEt₂ with [H(OEt₂)₂][BAR'₄] (Ar' = 3,5-(CF₃)₂C₆H₃) in diethyl ether at -78 °C is reported to produce a stable ethylene hydride product, (diimine)Pt(H)(η²-C₂H₄),⁶ the analogous reaction of (dfepe)PtEt₂ with the arenium acid [C₆Me₃H₄]⁺(B(C₆F₅)₄)⁻ in a 1:1 mixture of CD₂Cl₂ and DFB at -60 °C was examined. Ethane loss and the formation of a primary (dfepe)Pt product with a ³¹P resonance at δ 78.4 (¹J_{PtP} = 3330 Hz) and a partially-resolved shoulder at δ 79.5 was observed, which upon warming to -40 °C collapsed to a single broad resonance at δ 79.0. ¹H NMR spectra from -60 to +10 °C showed a range of broad poorly-defined resonances between 0 – 2 ppm. No clear evidence supporting the formation of either an ethylene hydride or agostic ethyl complex was obtained.

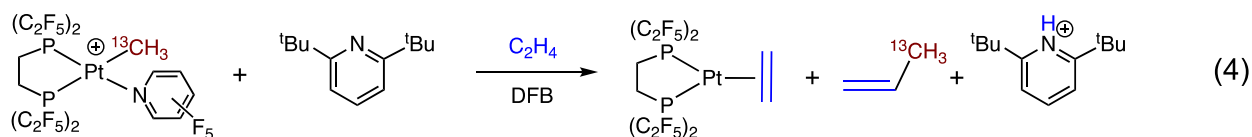
c) Hydride Trapping Studies. In our initial 2008 report we observed that the catalyst resting state (dfepe)Pt(Et)(η²-C₂H₄)⁺ converted upon consumption of available ethylene to a mixture of Pt(0) alkene species (dfepe)Pt(η²-alkene), presumably due to proton transfer from acidic (dfepe)Pt(H)(alkene)⁺ intermediates to more basic (relative to ethylene) butene products. To probe the Brønsted acidity of platinum hydride intermediates, the effect of added proton traps was investigated. Tilley and coworkers have reported Me₃SiPh and Me₃SnPh as efficient non-nucleophilic proton traps for an electrophilic Pt(II) bis-triflate hydroamination system.¹³ However, the presence of 1.2

equiv. Me_3SiPh did not affect the rate of butene product formation by $(\text{dfepe})\text{Pt}(\text{Me})(\text{NC}_5\text{F}_5)^+$ under standard catalyst conditions, and addition of 1.2 equiv. Me_3SnPh to $(\text{dfepe})\text{Pt}(\text{Me})(\text{NC}_5\text{F}_5)^+$ in *o*-difluorobenzene instead resulted in methylation to form $(\text{dfepe})\text{Pt}(\text{Me})_2$.

Typical proton traps are sterically-hindered amines which have high proton affinities combined with low nucleophilicity toward sterically-hindered Lewis acid sites. 2,2,6,6-tetramethylpiperidine, 2,6-diphenylpyridine and triethylamine were found to be ineffective and gave uncharacterized products when added to solutions of $(\text{dfepe})\text{Pt}(\text{Me})(\text{NC}_5\text{F}_5)^+$ in *o*-difluorobenzene. Addition of 1.2 equivalents of 2,6-lutidine to a solution of $(\text{dfepe})\text{Pt}(\text{Me})(\text{NC}_5\text{F}_5)^+$ in *o*-difluorobenzene resulted in pentafluoropyridine displacement to yield $[(\text{dfepe})\text{Pt}(\text{Me})(2,6\text{-lutidine})]^+$, tentatively identified by ^{31}P NMR (δ 76.3, $^1J_{\text{PtP}} = 1340$ Hz; trans to CH_3 , δ 62.6, $^1J_{\text{PtP}} = 4000$ Hz; trans to 2,6-lutidine). Finally, the more sterically-hindered base 2,6-di-*t*-butylpyridine, which has been extensively used as proton trap in living carbocationic polymerization systems,^{14,15} was examined. No significant changes in the spectra of **5** in *o*-difluorobenzene occurred upon addition of one equiv. 2,6-di-*t*-butylpyridine, indicating that 2,6-di-*t*-butylpyridine does not displace pentafluoropyridine from $(\text{dfepe})\text{Pt}(\text{Me})(\text{NC}_5\text{F}_5)^+$. Upon addition of ethylene, however, the clean stoichiometric production of 2,6-di-*t*-butylpyridinium, propene, and the neutral ethylene complex $(\text{dfepe})\text{Pt}(\text{C}_2\text{H}_4)$ was observed, consistent with efficient base interception of the hydride intermediates $(\text{dfepe})\text{Pt}(\text{H})(\text{alkene})^+$ or $(\text{dfepe})\text{Pt}(\text{H})(\text{sol}/\nu)^+$.

The initial formation of propene from $(\text{dfepe})\text{Pt}(\text{Me})(\text{C}_2\text{H}_4)^+$ during catalytic dimerization runs has also been verified by a ^{13}C labeling study: treatment of $[(\text{dfepe})\text{Pt}(^{13}\text{CH}_3)(\text{NC}_5\text{F}_5)]^+\text{B}(\text{C}_6\text{F}_5)_4^-$ with ethylene in the presence of 2,6-di-*t*-butylpyridine

cleanly afforded $(dfep)Pt(\eta^2-C_2H_4)$ and free $^{13}CH_3CH=CH_2$ (Equation 4), which was identified by ^{13}C NMR.



d) $(dfep)Pt(Me)(L)^+$ Ethylene Dimerization Kinetic Studies. The ethylene dimerization activity of $[(dfep)Pt(Me)(NC_5F_5)]^+B(C_6F_5)_4^-$ reported briefly in our previous paper has been examined in more detail. The activity of $[(dfep)Pt(Me)(NC_5F_5)]^+B(C_6F_5)_4^-$ was followed by 1H NMR under 600 psi ethylene (~ 175 equiv. dissolved ethylene) at $27^\circ C$ using a previously-described sapphire NMR sample tube assembly.¹⁶ The deviation from linearity noted prior to the 10 minute mark is due to the initial conversion of $[(dfep)Pt(Me)(C_2H_4)]^+$ to propene and the active catalyst resting state, $[(dfep)Pt(Et)(C_2H_4)]^+$ (**Figure 3**). The measured steady-state rate of 2-butenes (trans:cis $\sim 2:1$) production of $0.700(5) \text{ mol}^{-1} \text{ min}^{-1}$ corresponds to a $\Delta G^\ddagger(300 \text{ K})$ of $20.2(1) \text{ kcal mol}^{-1}$, considerably less than that reported for $(diimine)Pt(Et)(C_2H_4)^+$ ($\Delta G^\ddagger(373 \text{ K}) = 29.8 \text{ kcal mol}^{-1}$).⁶

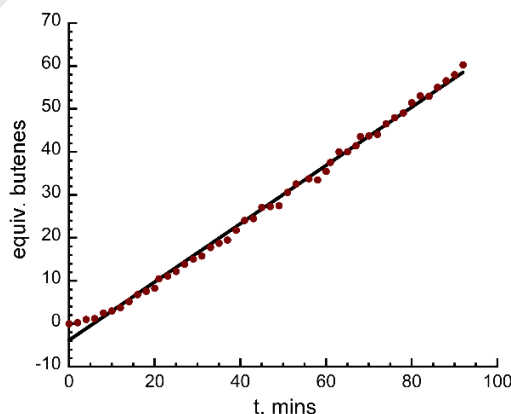


Figure 3. Plot of butenes production by $[(dfep)Pt(Me)(NC_5F_5)]^+B(C_6F_5)_4^-$ in *o*-difluorobenzene (0.018 M) under 600 psi (~ 175 equiv., 3.2 M) ethylene at $27^\circ C$. The rate of butenes production excluding the initial 10 mins. of data was $0.700(5) \text{ mol}^{-1} \text{ min}^{-1}$.

The catalytic activity of $[(\text{dfepe})\text{Pt}(\text{Me})(\text{NC}_5\text{F}_5)]^+\text{B}(\text{C}_6\text{F}_5)_4^-$ was also measured at -10, 0 and +10 °C in the presence of excess ethylene (see Supplementary Materials for 0 and +10 °C kinetic plots). As shown in **Figure 4, Plot (a)**, significant non-linearity is apparent at -10 °C due to the competitive conversion of $[(\text{dfepe})\text{Pt}(\text{Me})(\text{C}_2\text{H}_4)]^+$ under these conditions to the $[(\text{dfepe})\text{Pt}(\text{Et})(\text{C}_2\text{H}_4)]^+$ catalyst resting state. Monitoring by ^{31}P NMR gave a first-order rate constant for this conversion step of $k_{\text{init}} = 0.0022(4) \text{ min}^{-1}$, corresponding to a ΔG^\ddagger of 20.7 kcal mol $^{-1}$ for ethylene insertion into the Pt-Me bond. Applying this correction (dividing butenes production by the $[\text{Pt}(\text{Et})]/[\text{Pt}(\text{Me})]_0$ ratio as a function of time) gave **Plot 4b** with an associated rate of $0.00638(6) \text{ min}^{-1}$ with a slightly lower ΔG^\ddagger of 20.1 kcal mol $^{-1}$ for ethylene insertion into the Pt-Et bond. The limited stability of $[(\text{dfepe})\text{Pt}(\text{Et})(\text{NC}_5\text{F}_5)]^+\text{B}(\text{C}_6\text{F}_5)_4^-$ prevented us from directly examining dimerization kinetics without the added complication of Pt-Me to Pt-Et conversion.

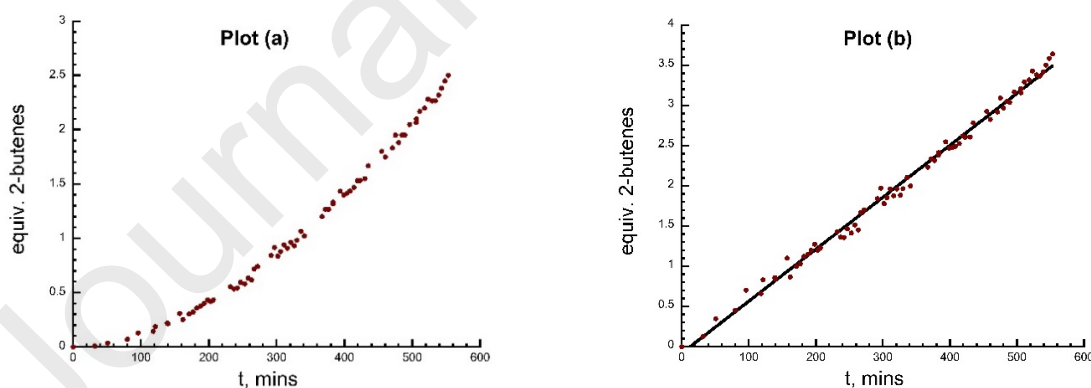


Figure 4. Plot (a): Uncorrected plot of 2-butenes production by $\{[(\text{dfepe})\text{Pt}(\text{Me})(\text{NC}_5\text{F}_5)]^+\text{B}(\text{C}_6\text{F}_5)_4]^-\}$ (0.014 M) in *o*-difluorobenzene in the presence of 23 equivs. ethylene at -10 °C. Plot (b): 2-butenes production divided by catalyst fraction $[\text{Pt}(\text{Et})]/[\text{Pt}(\text{Me})]_0$, calculated from $[\text{PtEt}] = [\text{PtMe}]_0 e^{-kt}$, with $k = 0.0022(4) \text{ min}^{-1}$, giving an effective conversion rate of $0.00638(6) \text{ min}^{-1}$.

The kinetic order in ethylene was examined by monitoring the initial rate of butene formation as a function of ethylene concentration. Monitoring butenes production at 27 °C by $[(\text{dfepe})\text{Pt}(\text{Me})(\text{NC}_5\text{F}_5)]^+\text{B}(\text{C}_6\text{F}_5)_4^-$ in *o*-difluorobenzene in the presence of 12 and 175 equiv. ethylene revealed only a slight difference in activity during the initial conversion to the Pt-ethyl catalyst resting state, but a significant difference in activity (~ 3 -fold) under high ethylene concentration (**Figure 5**). This unusual behavior differs from the ethylene-independent rate observed previously for $(\text{diimine})\text{Pt}(\text{Et})(\text{C}_2\text{H}_4)^+$.⁶ Control of ethylene concentration throughout our studies was problematic: variation of ethylene condensation into 5 mm NMR tubes was sensitive to time and mixing. At the highest concentrations (i.e., 175 equiv.) this introduces ethylene concentration-dependent kinetic behavior, but at lower concentrations the assumption of ethylene independence and rate-determining ethylene insertion appears to be reasonable (see below).

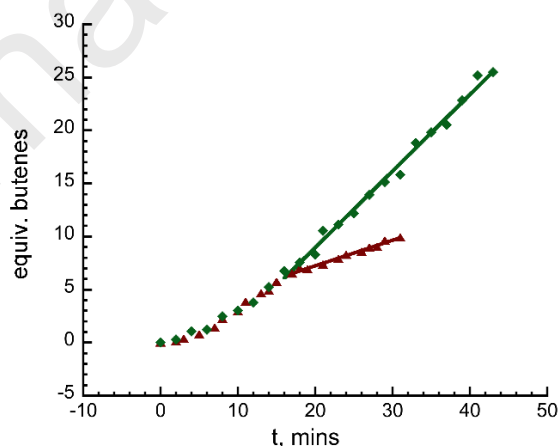


Figure 5. Ethylene dependence of butenes production by $\{(\text{dfepe})\text{Pt}(\text{Me})(\text{NC}_5\text{F}_5)^+\text{B}(\text{C}_5\text{F}_6)_4^-\}$ (0.018 M) in *o*-difluorobenzene in the presence of 12 equiv. (\blacktriangle , 0.22 M,) and 175 equiv. (\blacklozenge , 3.2 M, $0.700(5) \text{ min}^{-1}$) ethylene at 27 °C. Rates taken from the linear regions after 16 min. are $0.241(8) \text{ min}^{-1}$ and $0.700(5) \text{ min}^{-1}$, respectively.

An Eyring plot of -10, 0, 10, and 27 °C data is revealing (**Figure 6**): The rate dependence under limited amounts (6 - 23 equiv.) of ethylene is well-behaved, but the increased butenes production rate under high ethylene concentration is a significant outlier and suggests a competing associative pathway. The obtained activation values of $\Delta H^\ddagger = +15.4(1)$ kcal mol⁻¹ and $\Delta S^\ddagger = -7.0(5)$ EU are in reasonable agreement with DFT calculated values for ethylene insertion into the Pt-Me bond of the model complex $[(CF_3)_2PCH_2CH_2P(CF_3)_2]Pt(Me)(C_2H_4)]^+$ of $\Delta H^\ddagger = +19.9(1)$ kcal mol⁻¹ and $\Delta S^\ddagger = -7.1$ EU (see later).

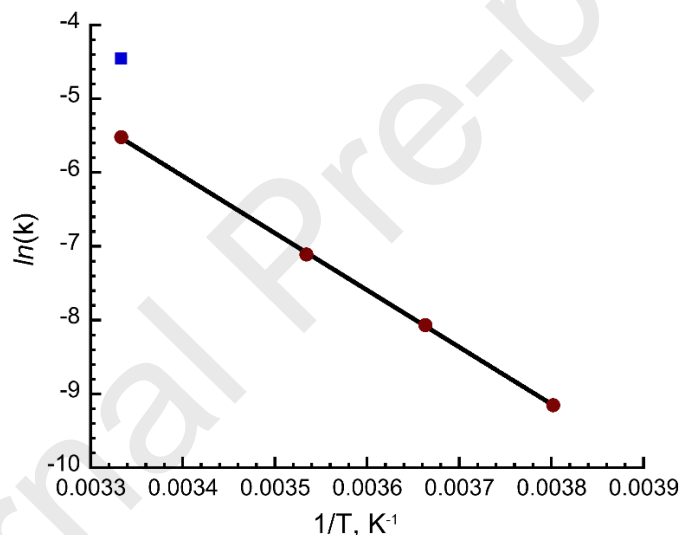


Figure 6. Eyring plot of ethylene dimerization activity by $\{(dfepe)Pt(Me)-(NC_5F_5)^+\}B(C_5F_6)_4^-$ under limited ethylene (●, 2-23 equiv.), showing the outlier data at 27 °C with 175 equiv. ethylene (■).

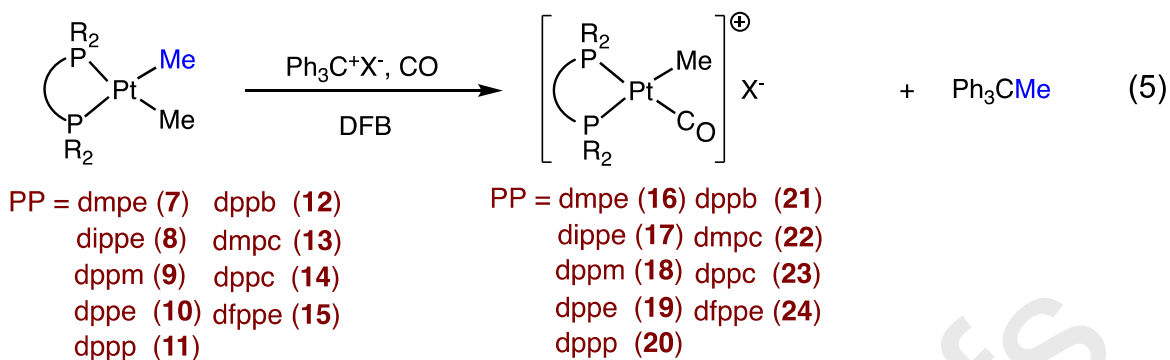
(PP)Pt(Me)(L)⁺ Chemistry

There is an unresolved question in $(dfepe)Pt(Me)(L)^+$ chemistry: Is the dramatic ethylene dimerization catalytic rate enhancement achieved by replacing the diimine ancillary ligand by dfepe unique to PFAP ligands, or a more general feature in phosphine

catalyst analogues? To address this issue, we have prepared a broad range of diphosphine platinum systems and examined their catalytic activity.

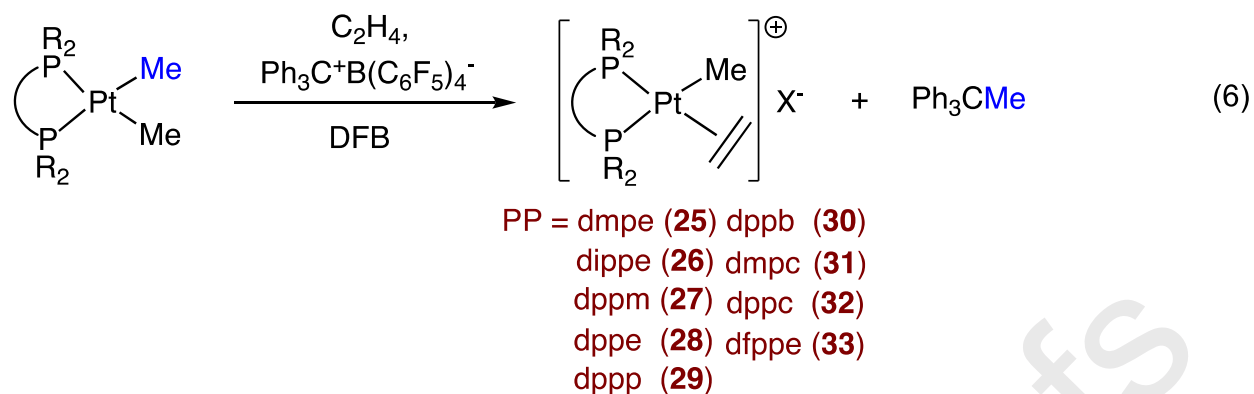
a) (PP)PtMe₂ Syntheses. A series of (PP)PtMe₂ diphenylphosphine complexes with varying chelate backbone length (dppm, dppe, dppp, dppb), as well as the methyl- and isopropyl-substituted C₂-bridged chelates dmpe and dippe are readily prepared from (cod)PtMe₂ and the appropriate diphosphine.¹⁷ (dfppe)PtMe₂, previously prepared by methylation of (dfppe)PtCl₂,¹⁸ was prepared in a similar manner from (cod)PtMe₂, as were the dimethyl complexes incorporating the carboranyl backbone chelates 1,2-bis(dimethylphosphino)carborane (dmpe) and 1,2-bis(diphenylphosphino)carborane (dppc). The diphosphines examined in this study are summarized in Chart 1.

b) (PP)PtMe(CO)⁺ Syntheses. $\nu(\text{CO})$ values provide useful qualitative information on relative net metal electron density for the diphosphine systems used in this study (Table 1). Methyl abstraction from (PP)PtMe₂ precursors by the trityl cation, [Ph₃C]⁺B(C₆F₅)₄⁻,¹⁹ in the presence of 1 atm CO in the polar poorly-coordinating solvent *o*-difluorobenzene (DFB) is a convenient route to the corresponding donor phosphine carbonyl cations (PP)Pt(Me)(CO)⁺ (Equation 5). In the case of (dppm)PtMe₂, abstraction using [Ph₃C]⁺B(C₆F₅)₄⁻ under CO didn't produce the expected monomeric product (dppm)Pt(Me)(CO)⁺ (**18**), but rather a single major (~65%) species that has been tentatively assigned as the bimetallic complex [(μ -dppm)₂Pt₂(Me)₂(CO)]²⁺.²⁰ Carbonyl complex **18** was obtained as a minor component using [Ph₃C]⁺SbF₆⁻ as the methyl abstraction reagent and was characterized by ³¹P NMR and IR. [(dippe)Pt(Me)(CO)]⁺B(C₆F₅)₄⁻ (**17**) has been crystallographically characterized (see Supplemental Section).



No corresponding methyl abstraction by trityl cation from the perfluoroalkylphosphine (PFAP) derivative (dfepe)PtMe₂ occurs in the presence of CO, presumably due to its significantly reduced metal electron density, but (dfepe)Pt(Me)(CO)⁺ has been prepared by CO substitution of [(dfepe)PtMe(NC₅F₅)]⁺B(C₆F₅)₄⁻,⁸ or by methyl abstraction in the presence of CO using the more powerful SbF₅(SO₂) reagent.²¹

c) (PP)PtMe₂ Ethylene Dimerization Studies. In contrast to the dfepe system, which is accessed via the labile pentafluoropyridine adduct (dfepe)Pt(Me)(NC₅F₅)⁺, the corresponding donor phosphine catalyst systems are more conveniently accessed by direct methyl abstraction with trityl cation in the presence of ethylene to form *in situ* (PP)Pt(Me)(C₂H₄)⁺ products (Equation 6). For (dfepe)PtMe₂, trityl abstraction in the presence of ethylene is very slow and not quantitative (see later). Continued exposure to excess ethylene at ambient temperatures results in conversion to the corresponding ethyl complexes, (PP)Pt(Et)(C₂H₄)⁺. A general trend noted for all examined (PP)Pt(Me)(C₂H₄)⁺/ (PP)Pt(Et)(C₂H₄)⁺ pairs is a consistent increase in ¹J_{PtP} of 160 – 360 Hz for the phosphorus trans to the ethylene ligand and decrease of 140 – 170 Hz for the phosphorus trans to the alkyl ligand going from the methyl to the ethyl complexes.



Initial Pt-methyl ethylene insertion rates and ethylene dimerization activities of the complexes **25** – **33** were evaluated by ^1H NMR under excess (20 - 90 equiv.) ethylene in DFB and are summarized in Table 1, along with the time dependent distribution of butene products. Dimerization activities span a ~30-fold range of activity from 0.06 TO/hr for (dmpe)Pt(Et)(C₂H₄)⁺ to 1.90 TO/hr for the perfluoroaryl complex (dfppe)Pt(Et)(C₂H₄)⁺. For (dppm)Pt(Me)(C₂H₄)⁺ the disappearance of the Pt-Me resonance could be monitored, but the dimerization activity could not be determined due to the competitive appearance of a new species with a ^{31}P resonance at -1.6 ppm which we tentatively assign as the bimetallic complex [(μ-dppm)₂Pt₂(Me)₂(C₂H₄)₂]²⁺ based on its similarity to the analogous carbonyl adduct [(μ-dppm)₂Pt₂(Me)₂(CO)₂]²⁺.¹²

The activity of (dppe)Pt(Et)(C₂H₄)⁺ is anomalous: after three days, broad ^1H NMR resonances at δ 1.2 and 0.8 begin to appear due to oligomerized ethylene, and after the complete consumption of all ethylene in 7 days a ~1:1 integrated mixture of butenes and oligomeric product is obtained; this behavior is similar to that observed for (dfepe)Pt(Et)(C₂H₄)⁺ and has been attributed previously to acid catalysis rather than multiple insertion chemistry. No oligomerization activity is observed for any of the other diphosphine systems examined.

Unlike the (dfepe)Pt(Me)(C₂H₄)⁺ system, which generates isomerized 2-butene as the sole observed product, significant amounts of 1-butene are observed in all donor phosphine systems; over time the ratio of 2-butenes/1-butene was found to increase in all cases. The penultimate accepting phosphine system (dfppe)Pt(Me)(C₂H₄)⁺ most closely approaches the behavior of (dfepe)Pt(Me)(C₂H₄)⁺ both in terms of dimerization and butene isomerization activity.

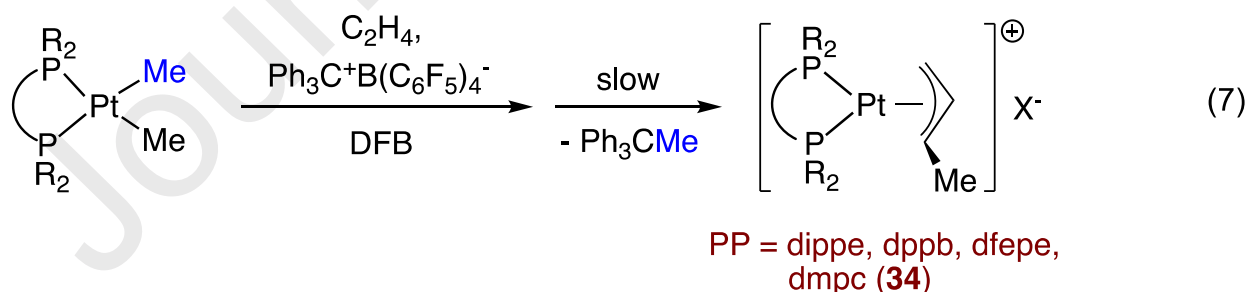
Table 1. Summary of (PP)Pt(Me)(L)⁺ (L = CO, C₂H₄) comparative data

diphosphine system	(PP)Pt(Me)(L) ⁺ ν(CO) (cm ⁻¹ , DCM solvent)	Pt-Me insertion rate, hr ⁻¹ (22 °C, DFB solvent)	Total butenes activity, TOF hr ⁻¹ (22 °C, DFB solvent)	% selectivity for 2-butenes (elapsed hours)
dmpe	2112	0.00176(5)	0.06(1)	36(191), 60(408)
dippe	2106	0.115(1)	0.32(3)	54(46)
dppm	2110	0.00248(3)	---	---
dppe	2114	0.0422(3)	0.07(1)	53(47), 90(168)
dppp	2117	0.169(2)	0.24(2)	77(4), 97(284)
dppb	2118	0.107(1)	0.45(4)	79(16), 93(46)
dmpc	2132	0.413(8)	0.68(3)	92(19), 98(41)
dppc	2133	0.45(1)	0.94(9)	55(19), 84(71)
dfppe	2149	1.63(3)	1.90(10)	85(21), 96(28)
dfepe	2174 ⁸	---	42.0(3) ^a	100

^aThis study, T = 27 °C.

d) (PP)Pt(η³-C₃H₄Me)⁺ formation from (PP)Pt(Et)(C₂H₄)⁺. As was observed for (dfepe)Pt(Et)(C₂H₄)⁺, the (PP)Pt(Et)(C₂H₄)⁺ catalyst resting states for all other phosphine systems examined persist in the presence of excess ethylene. The ultimate fate of the catalyst after ethylene consumption, however, is variable. The majority of diphosphine

systems decompose to uncharacterized platinum product mixtures. In the cases where PP = dppb, dmpe, and dippe, however, conversion to a single major product occurred. The products formed from dppb and dippe were only partially characterized: single broad ^{31}P resonances were observed with $^1J_{\text{PtP}} = 3530$ and 3520 Hz, respectively, and the corresponding ^1H NMR spectra exhibited only a series of broad features between 0 and 2 ppm (apart from the 1- and 2-butene product resonances) and new methyl singlets. The behavior of $(\text{dmpe})\text{Pt}(\text{Et})(\text{C}_2\text{H}_4)^+$ was more definitive: 12 hrs after consumption of ethylene a clean (~95%) conversion to a single product was indicated by the appearance of an AB set of ^{31}P resonances at 47.3 ppm ($J_{\text{PP}} = 15.5$ Hz) with very similar $^1J_{\text{PtP}}$ values (3732, 3722 Hz). Isolation of single crystals from the dmpe product solution and characterization by X-ray diffraction showed this product to be the 1-methylallyl product $[(\text{dmpe})\text{Pt}(\eta^3\text{-C}_3\text{H}_4\text{Me})]^+\text{B}(\text{C}_6\text{F}_5)_4^-$ (**34**) (Equation 7, **Figure 7**). From this result we conclude that the single ^{31}P resonances observed for the dppb and dippe catalyst products are likely due to isochronous (or dynamically exchanged) P centers in analogous $(\text{dppb})\text{Pt}(\eta^3\text{-C}_3\text{H}_4\text{Me})^+$ and $(\text{dippe})\text{Pt}(\eta^3\text{-C}_3\text{H}_4\text{Me})^+$ products.



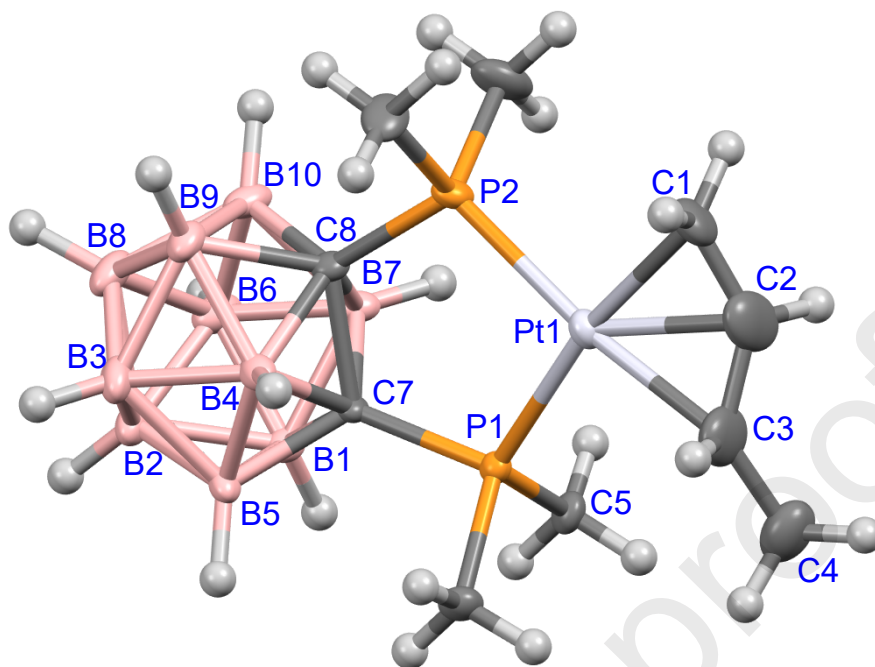
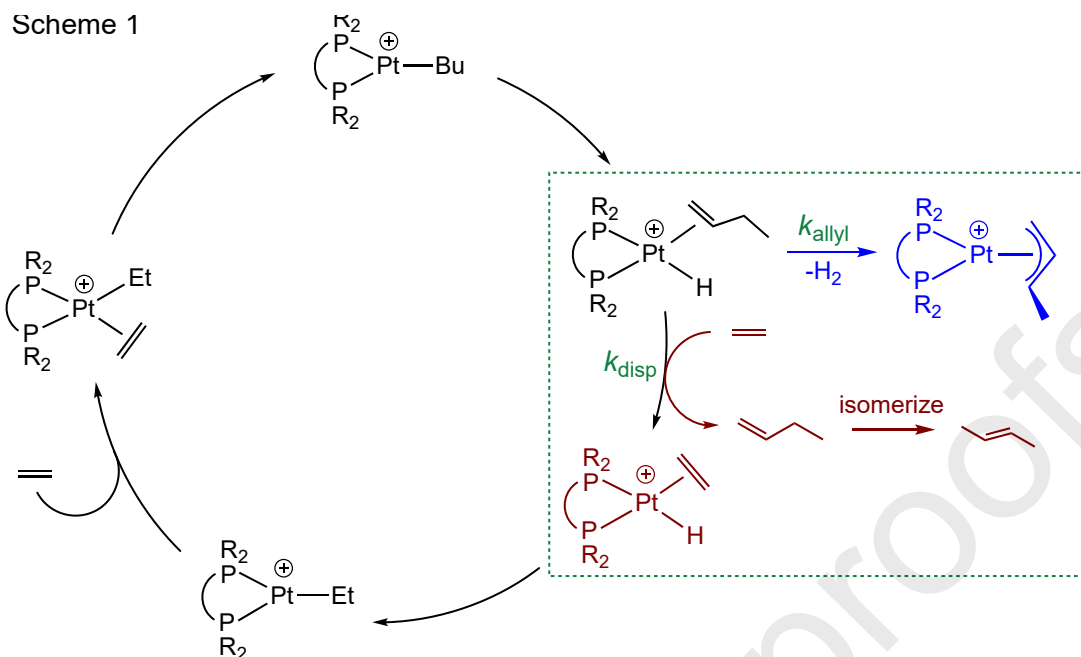


Figure 7. Crystal structure of $[(dmpe)Pt(\eta^3-C_3H_4Me)]^+B(C_6F_5)_4^-$ (**34**) with thermal ellipsoids at the 35% probability level. The borate anion is not shown. Selected metrical data (bond lengths in Å and angles in deg): Pt(1)-C(1): 2.197(6); Pt(1)-C(2): 2.147(7); Pt(1)-C(3): 2.229(7); Pt(1)-P(1): 2.247(1); Pt(1)-P(2): 2.238(1); P(1)-Pt(1)-C(1): 168.9(2); P(1)-Pt(1)-C(3): 100.7(2); P(2)-Pt(1)-C(1): 98.3(2); P(2)-Pt(1)-C(3): 164.7(3).

Interestingly, although attempts to directly access $(dfepe)Pt(R)(C_2H_4)^+$ products from trityl methyl abstraction from $(dfepe)PtMe_2$ in the presence ethylene were unsuccessful, after prolonged standing crystals of the corresponding methylallyl complex $[(dfepe)Pt(\eta^3-C_3H_4Me)]^+B(C_6F_5)_4^-$ (**35**) were obtained and also crystallographically characterized (see Supplementary Section). A tentative mechanism to account for the formation of these allylic products is shown in Scheme 1. Overlaid on the standard ethylene dimerization mechanism is a competition between associative interchange (k_{disp}) of butene with ethylene, which continues the dimerization pathway, and irreversible allylic activation (k_{allyl}) of the intermediate butene adduct. As long as a sufficient concentration of ethylene persists, the allylic deactivation step is suppressed.



DFT modeling of ethylene insertion barriers.

A key issue to consider is: why are platinum diphosphine catalysts generally more active than the corresponding diimine system? To probe this question, the barriers to ethylene insertion for Brookhart's diimine catalyst and a range of model PP chelate systems have been evaluated by DFT methods (M06l functional, def2 basis sets). A comparative natural bond order (NBO) analysis of the model perfluoroalkylphosphine complex $(dfmpe)Pt(Me)(C_2H_4)^+$ ($dfmpe = (CF_3)_2PCH_2CH_2P(CF_3)_2$) versus (diimine) $Pt(Me)(C_2H_4)^+$ (diimine = $[(2,6-Me_2C_6H_3)N=C(An)-C(An)=N(2,6-Me_2C_6H_3)]$, An = 1,8-naphylenediyl)) has also been carried out. DFT results are summarized in Table 2.

Table 2. Summary of DFT results (M06l, def2 basis sets) for (PP)Pt(Me)(C₂H₄)⁺ and (diimine)Pt(Me)(C₂H₄)⁺ insertion barriers to form agostic Pt(C₃H₇)⁺ products (diimine = [(2,6-Me₂C₆H₃)N=C(An)-C(An)=N(2,6-Me₂C₆H₃)], An = 1,8-naphylenediyl).

ligand system	L ₂ Pt(Me)(C ₂ H ₄) ⁺ ΔG [‡] for insertion, kcal mol ⁻¹	L ₂ Pt(Me)(C ₂ H ₄) ⁺ ΔG for insertion, kcal mol ⁻¹	L ₂ Pt(Me)(C ₂ H ₄) ⁺ ΔG for C ₂ H ₄ binding, kcal mol ⁻¹
(dmpm)Pt	26.3	0.0	13.0
(dmpe)Pt	23.3	0.1	13.3
(dmpp)Pt	23.3	-2.0	12.3
<i>cis</i> -(Me ₃ P) ₂ Pt	23.2	-2.6	10.1
(dppe)Pt	25.1	1.9	14.8
(dfmpe)Pt	22.0	1.6	20.5
(diimine)Pt	30.1	12.9	33.4

Calculated activation barriers for (dfmpe)Pt(Me)(C₂H₄)⁺ (22.0 kcal mol⁻¹) and (diimine)Pt(Me)(C₂H₄)⁺ (30.1 kcal mol⁻¹) are in reasonable agreement with experimental values found for (dfepe)Pt(Et)(C₂H₄)⁺ (20.2(1) kcal mol⁻¹, 300 K) and (diimine)Pt(Et)(C₂H₄)⁺ (29.8 kcal mol⁻¹, 373 K). Insertion barriers for donor phosphine systems, with the exception of chelate-constrained (dmpm)Pt(Me)(C₂H₄)⁺, are slightly higher than found for the dfmpe model complex and are insensitive to chelate chain length or replacement by unconstrained Me₃P groups. The high insertion barrier for (diimine)Pt(Me)(C₂H₄)⁺ correlates with a significantly higher ethylene binding energy than donor phosphine analogues (33.4 vs. 10.1 – 14.8 kcal mol⁻¹), which should contribute to stabilization of the reactant ground state. Interestingly, the ethylene bonding energy for (dfmpe)Pt(Me)(C₂H₄)⁺ (20.5 kcal mol⁻¹) is significantly *higher* than in donor phosphine complexes despite the lower overall insertion barrier. This might reflect reduced ethylene backbonding counterbalanced by a weaker phosphine trans-influence and greater sigma electrostatic attraction.

Some insight into relative ethylene insertion barriers into Pt-Me bonds is provided by calculated transition state geometries and relative bond orders (**Figure 8**). Overall, changes in bond lengths are very similar: for $(dfmpe)Pt(Me)(C_2H_4)^+$, Pt-Me bond-lengthening to form the 4-center transition state is 0.22 Å and the formed Pt-C(ethylene) bond length of 2.10 Å closely matches the reactant Pt-Me bond length. The corresponding values for $(diimine)Pt(Me)(C_2H_4)^+$ (0.21 Å lengthening, Pt-C(ethylene) = 2.03 Å) mirror these changes. Changes in spectator *dfmpe* and *diimine* ligated atom metal bond lengths (i.e., the trans influence) as the degree of Pt-C sigma bonding evolves is also similar: Elongated Pt-P and Pt-N bonds trans to Pt-Me (2.35, 2.20 Å, respectively) contract to 2.23 and 2.04 Å as the Pt-Me bond is partially broken, and the Pt-P and Pt-N bonds initially trans to Pt-ethylene elongate to a similar degree: Pt-P = 2.32, Pt-N = 2.20 Å.

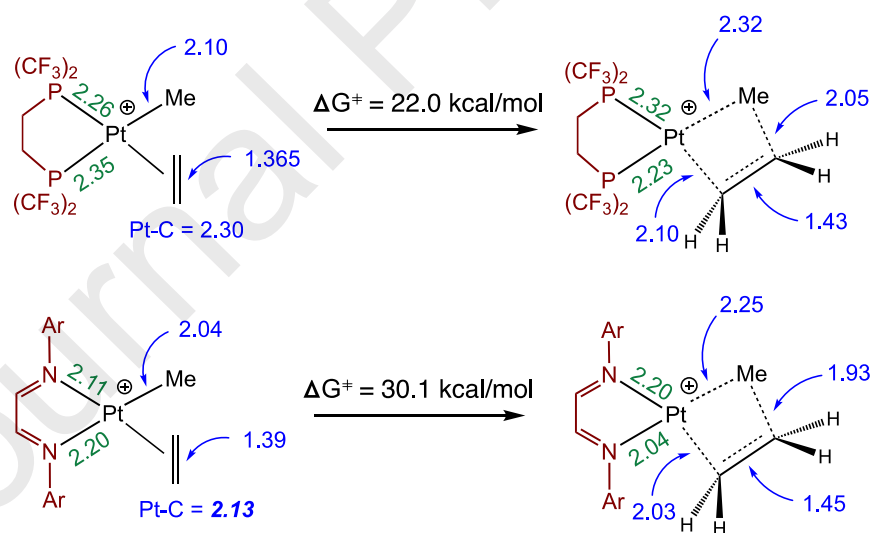


Figure 8. Selected metrical parameters (Å) for $(dfmpe)Pt(Me)(C_2H_4)^+$ and $(diimine)Pt(Me)(C_2H_4)^+$ reactant and transition state calculated geometries (DFT, M06l, def2 basis sets).

The most significant differences in the diphosphine and diimine complex approaches to the transition state are (1) The much shorter Pt-ethylene bond lengths for the diimine complex (2.13 Å vs. 2.30 Å for $(dfmpe)Pt(Me)(C_2H_4)^+$), and (2) the shorter Me-ethylene bond length in the transition state for the diimine complex, 1.93 vs. 2.05 Å, indicative of more extensive Me migration to ethylene (i.e., a later transition state). Overall, while the bond-breaking cost for the Pt-Me bond lost is effectively counterbalanced by Pt-C(ethylene) sigma bond formation in both ligand systems, the loss of the stronger binding energy of $(diimine)Pt(Me)^+$ to ethylene (33.4 kcal mol⁻¹) compared to the 20.5 kcal mol⁻¹ binding energy for $(dfmpe)Pt(Me)^+$ could explain the difference in insertion barriers. This can be rephrased in classic coordination chemistry terms: the greater trans-influence of ancillary phosphine ligands relative to diimine ligands substantially weakens ethylene binding and raises the reactant ground state energy.

Changes in bonding energetics can also be evaluated by considering Wiberg bond order indices,²² which are available from natural bond order analysis. For $(dfmpe)Pt(Me)(C_2H_4)^+$, the calculated index for the Pt-C(ethylene) bonds is 0.350, which diverges at the transition state to 0.574 (sigma bond forming to Pt) and 0.174 (sigma bond forming to migrating Me). For $(diimine)Pt(Me)(C_2H_4)^+$, however, the calculated index for the Pt-C(ethylene) bonds is significantly higher, 0.522, and diverges in the transition state to 0.703 (sigma bond forming to Pt) and 0.167 (sigma bond forming to migrating Me). The “bond order gain” in forming the new Pt-C sigma bond for $(dfmpe)Pt(Me)(C_2H_4)^+$ (+0.224) is higher than the +0.181 gain for $(diimine)Pt(Me)(C_2H_4)^+$. In other words, there is an energetic advantage in forming a new Pt-C sigma bond from the more weakly-bound

ethylene ligand in $(dfmpe)Pt(Me)(C_2H_4)^+$ relative to the same ethylene insertion process for $(diimine)Pt(Me)(C_2H_4)^+$.

Summary

Building upon our initial reported work for the special case of PP = perfluoroalkylphosphine, this paper more generally establishes that $(PP)Pt(alkyl)(ethylene)^+$ systems are significantly more activated toward migratory insertion relative to $(diimine)Pt(alkyl)(ethylene)^+$. Further $(dfepe)Pt(R)(L)^+$ investigations have (a) demonstrated more labile adducts, (b) confirmed $(dfepe)Pt(Et)(C_2H_4)^+$ as the catalyst resting state, and (c) verified propene as the initial product following Pt-Me insertion. Base trapping studies with 2,6-di-*t*-butylpyridine implicate the intermediacy of acidic hydride intermediates in the ethylene dimerization catalytic cycle.

Kinetics studies confirm the significantly lower insertion barrier for $(dfepe)Pt(Et)(C_2H_4)^+$ (20.2(1) kcal mol⁻¹) relative to $(diimine)Pt(Et)(C_2H_4)^+$ (29.8 kcal mol⁻¹), and variable temperature kinetics gave activation values ($\Delta H^\ddagger = +15.4(1)$ kcal mol⁻¹ and -7.0(5) EU) in reasonable agreement with calculated values. Under moderate amounts of excess ethylene, the rate of dimerization is zero-order in alkene but at higher pressures a modest but significant rate acceleration is observed which suggests a competing associate reaction pathway.

A broad range of phosphine chelate systems $(PP)Pt(Me)(C_2H_4)^+$ have been prepared *in situ* by trityl abstraction of methyl from $(PP)PtMe_2$ in the presence of ethylene and their activity has been examined (Table 1). No other diphosphine system approaches PP = dfepe in activity, but a clear trend of increased activity with decreasing diphosphine donor ability is established: $\nu(CO)$ data confirm that the most active dimerization catalysts

(PP = dmpe, dppe, dfppe, dfepe) are also the most electron poor. Beyond the low activity of the highly constrained (dppm)Pt chelate, a modest increase in activity follows increasing chelate chain length (dppe, dppp, dppb). Steric influence is best demonstrated by the (dippe)Pt(Me)(C₂H₄)⁺ system, which is ~65 times more active toward insertion into the Pt-Me bond than (dmpe)Pt(Me)(C₂H₄)⁺. Several instances where catalyst decomposition to an inactive allylic final product have been noted, exemplified most clearly by structurally-characterized (dmpe)Pt(η³-C₃H₄Me)⁺.

DFT studies have been carried out in order to shed light on the (diphosphine)Pt versus (diimine)Pt activity issue (Table 2). All propyl insertion products exhibit a modest degree of agostic binding of the pendant methyl group. Calculated Pt-Me insertion barriers agree well with the experimentally-determined barrier for (dfepe)Pt(Et)(C₂H₄)⁺ and the reported value for (diimine)Pt(Et)(C₂H₄)⁺. Only slight differences in insertion barriers for donor phosphine systems are found; all donor phosphine systems have calculated ethylene binding energies between 10 and 15 kcal mol⁻¹. The only outliers in ethylene binding energy happen to be the most active (dfepe) and least active (diimine) analogues; both of these have significantly higher ethylene ligand binding energies. The diimine system is also an outlier in ΔG for the insertion process: whereas all diphosphine systems are close to thermoneutral, ΔG for (diimine)Pt(Me)(C₂H₄)⁺ is +12.9 kcal mol⁻¹. Qualitatively, the higher barrier for ethylene insertion for the diimine system can be attributed to a later transition state and the accompanying loss of strong Pt-ethylene binding.

In summary, the lower insertion barrier noted for diphosphine systems relative to diimine systems can be reduced down to a simple “back of the envelope” explanation that is rooted in well-known coordination chemistry trends: symmetric chelating strong-field and weak-field ancillary ligand trans binding sites are both thermoneutral with respect to the conversion of a reactant Pt-alkyl bond into a product Pt-alkyl bond. However, the conversion of a Pt-ethylene binding site to a weak Pt--(agostic γ -Me) binding site is *not* thermoneutral: stronger Pt-ethylene binding trans to a weak-field ligand (such as diimine) leads to an energetically uphill process which effects the activation barrier to insertion. We suggest that further explorations of ligand field effects, particularly in square planar group 10 catalyst systems, would be a worthwhile undertaking.

Experimental

General Procedures. All manipulations were conducted under N₂ or vacuum using high-vacuum line and glovebox techniques unless otherwise noted. All ambient pressure chemistry was carried out under a pressure of approximately 590 torr (elevation ~2195 m). All solvents were dried using standard procedures and stored under vacuum. Aprotic deuterated solvents used in NMR experiments were dried over activated 3 Å molecular sieves. Elemental analyses were performed by ALS Environmental. IR spectra were recorded on a Varian FTS-800 FTIR instrument. NMR spectra were obtained with a Bruker Avance-III-400 instrument using 5 mm NMR tubes fitted with Teflon valves (New Era Enterprises, Inc., NE-CAV5). Spectra taken in *o*-difluorobenzene were externally locked and referenced to acetone-*d*₆ capillaries (acetone-*d*₅ set to 2.07 ppm). ³¹P spectra were referenced to an 85% H₃PO₄ external standard. ¹⁹F spectra were referenced, to a CF₃CO₂CH₂CH₃ (-75.32 ppm) external standard. *o*-difluorobenzene (DFB),

pentafluoropyridine, pentafluorobenzonitrile, pentafluoroaniline, and pentafluoro-nitrobenzene were purchased from Synquest Labs, Inc. All other reagents, unless otherwise noted, were purchased from Aldrich and were used without further purification. $[(dfepe)Pt(Me)(NC_5F_5)]^+B(C_6F_5)_4^-$,⁸ $(cod)PtMe_2$,²³ $(dippe)PtMe_2$,^{17b}, $(dmpe)PtMe_2$,²⁴ $(PP)PtMe_2$ (PP = *dppm*, *dppe*, *dppp*, *dppb*),^{17a, 17c, 17d} 1,2-bis(diphenylphosphino)carborane (*dppc*),²⁵ 1,2-bis(dimethylphosphino)carborane (*dmpc*),²⁶ $[C_6Me_3H_4]^+(B(C_6F_5)_4)^-$,²⁷ $[Ph_3C]^+B(C_6F_5)_4^-$,¹⁹ $[Ph_3C]^+SbF_6^-$,²⁸ and $(dfepe)PtEt_2$ ⁷ were prepared following literature procedures. The synthesis of $^{13}CH_3Li$ is described in the Supplementary Section.

$[(dfepe)Pt(Me)(NCC_6F_5)]^+B(C_6F_5)_4^-$ (2**)**. 20 mg of $(dfepe)Pt(Me)(NC_5F_5)^+B(C_6F_5)_4^-$ and 1 mL of NCC_6F_5 were placed in a NMR tube fitted with a Teflon valve and heated at 80 °C for half an hour. Upon cooling to room-temperature, colorless crystals were deposited along the walls of the NMR tube and were collected for X-ray diffraction (see Supplemental Section). NMR data for the remaining solution were consistent with the clean formation of $[(dfepe)Pt(Me)(NCC_6F_5)]^+B(C_6F_5)_4^-$ (**2**). Preparatory-scale isolation of **2** was not attempted. 1H NMR (*o*-difluorobenzene, 400.13 MHz, 27 °C, external acetone-*d*₆ reference): δ 2.03 (m, 2H; *PCH*₂), 1.72 (m, 2H; *PCH*₂), 0.18 (br. s, $^2J_{PtH} = 43$ Hz, 3H; *PtCH*₃). ^{31}P NMR (*o*-difluorobenzene, 161.70 MHz, 27 °C): δ 79.9 (m, $^1J_{PtP} = 1490$ Hz, P trans to *CH*₃), 58.4 (m, $^1J_{PtP} = 4940$ Hz, P trans to NCC_6F_5).

$[(dfepe)Pt(Me)(NH_2C_6F_5)]^+B(C_6F_5)_4^-$ (3**)**. To a 5 mm NMR tube fitted with a Teflon valve containing 15 mg of $(dfepe)Pt(Me)(NC_5F_5)^+B(C_6F_5)_4^-$ in 1 mL of *o*-difluorobenzene was added 2 mg (~3 equiv.) of pentafluoroaniline. NMR data for the resulting solution confirmed the formation of **3**. 1H NMR (*o*-difluorobenzene, 400.13 MHz, 27 °C): δ 1.97

(m, 2H; PCH₂), 1.75 (m, 2H; PCH₂), 0.10 (br. s, ¹J_{PtH} = 42 Hz, 3H; PtCH₃). ³¹P NMR (*o*-difluorobenzene, 161.70 MHz, 27 °C): δ 76.8 (m, ¹J_{PtP} = 1480 Hz; P trans to CH₃), 60.9 (m, ¹J_{PtP} = 4450 Hz; P trans to NCC₆F₅). ¹⁹F NMR (376.5 MHz, *o*-difluorobenzene, 27 °C): δ -80.8 (s, 6F; PCF₂CF₃), -81.4 (s, 6F; PCF₂CF₃), -108 to -112 (overlapping ABX multiplets, 8F; PCF₂CF₃), -133.7 (br. s, 8F; *o*-B(C₆F₅)₄⁻), -150.8 (br. s, 2F; C₆F₅NH₂), -153.6 (br. s, 1F; C₆F₅NH₂), -160.6 (br. s, 2F; C₆F₅NH₂), -165.0 (t, ³J_{FF} = 20 Hz, 4F; *p*-B(C₆F₅)₄⁻), -168.8 (m, 8F; *m*-B(C₆F₅)₄⁻).

[(dfepe)Pt(Me)(O₂NC₆F₅)]⁺B(C₆F₅)₄⁻ (4**).** 15 mL of pentafluoronitrobenzene was added to a flask charged with (dfepe)Pt(Me)₂ (0.24 g, 0.30 mmol) and (C₆Me₃H₄)⁺B(C₆F₅)₄⁻ (0.29 g, 0.36 mmol). After 2 h of stirring, the resulting pale-green solid **4** (0.385 g, 76.2%) was collected by filtration, and dried under vacuum. Anal. Calcd for C₄₁H₇BF₄₅NO₂P₂Pt: C, 29.52; H, 0.42; Anal. found: C, 29.60; H, 0.74; ¹H NMR (*o*-difluorobenzene, 400.13 MHz, 20 °C): δ 2.00 (m, 2H; PCH₂), 1.70 (m, 2H; PCH₂), 0.29 (br. s, *v*_{1/2} = 40 Hz, 3H, PtCH₃). ³¹P NMR (161.70 MHz, *o*-difluorobenzene, 20 °C): δ 83.8 (m, ¹J_{PtP} = 1600 Hz; P trans to CH₃) δ 53.6 (m, ¹J_{PtP} = 5480 Hz; P trans to O₂NC₆F₅). ¹⁹F NMR (376.5 MHz, *o*-difluorobenzene, 20 °C): δ -80.7 (s, 6F; PCF₂CF₃), -81.8 (s, 6F; PCF₂CF₃), -108 to -113 (overlapping ABX multiplets, 8F; PCF₂CF₃), -133.7 (br. s, 8F; *o*-B(C₆F₅)₄⁻), -134.5 (br. s, *v*_{1/2} = 250 Hz, 2F; C₆F₅NO₂), -157.0 (br. s, *v*_{1/2} = 250 Hz, 2F; C₆F₅NO₂ (*p*-C₆F₅NO₂ not observed), -165.0 (t, ³J_{FF} = 20 Hz, 4F; *p*-B(C₆F₅)₄⁻), -168.8 (br. s, 8F; *m*-B(C₆F₅)₄⁻).

[(dfepe)Pt(Et)(NC₅F₅)]⁺B(C₆F₅)₄⁻ (5**).** To a flask charged with (dfepe)PtEt₂ (0.250 g, 0.305 mmol) and [C₆Me₃H₄]⁺(B(C₆F₅)₄)⁻ (0.370 g, 0.462 mmol) was added 15 mL of pentafluoropyridine. After stirring the mixture for 2 hrs the resulting white solid (0.470 g)

was collected by filtration and dried under vacuum. ^{19}F NMR spectra at $-40\text{ }^\circ\text{C}$ revealed 0.79 equiv. of unassociated pentafluoropyridine was present in the isolated product. Complex **5** has limited stability (hours) at ambient temperature, but may be stored indefinitely at $-25\text{ }^\circ\text{C}$. The limited instability of **5** precluded elemental analysis. ^1H NMR (400.13 MHz, ODFB, $-40\text{ }^\circ\text{C}$): δ 1.98 (m, 2H; PCH_2), 1.65 (m, 2H; PCH_2), 1.05 (m, br. ($\nu_{1/2} \sim 40\text{ Hz}$, 2H; PtCH_2CH_3), -0.24 (m, br. ($\nu_{1/2} \sim 30\text{ Hz}$, 2H; PtCH_2CH_3). ^{31}P NMR (161.70 MHz, ODFB, $-30\text{ }^\circ\text{C}$): δ 76.6 (pseudo pentet of doublets, $J_{\text{PP}} = 31\text{ Hz}$, $^2J_{\text{FP}} = 82\text{ Hz}$, $^1J_{\text{PtP}} = 1310\text{ Hz}$; P *trans* to Et), 56.4 (m, $^1J_{\text{PtP}} = 5240\text{ Hz}$, P *trans* to NC_5F_5). ^{19}F NMR (376.5 MHz, ODFB, $-40\text{ }^\circ\text{C}$): δ -80.9 (s, br., $^3J_{\text{PtH}} = 142\text{ Hz}$, 2F; *o*- NC_5F_5), -81.4 (s, 6F; PCF_2CF_3), -81.7 (s, 6F; PCF_2CF_3), -108 to -113 (overlapping ABX multiplets, 8F; PCF_2CF_3), -118.0 (m, 1F; *p*- NC_5F_5), -133.8 (m, 8F; *o*- $\text{B}(\text{C}_6\text{F}_5)_4$), -156.4 (m, 2F; *m*- NC_5F_5), -164.3 (t, $^3J_{\text{FF}} = 20\text{ Hz}$, 4F; *p*- $\text{B}(\text{C}_6\text{F}_5)_4$), -168.2 (m, 8F; *m*- $\text{B}(\text{C}_6\text{F}_5)_4$).

[(dfepe)Pt(Et)($\eta^2\text{-C}_2\text{H}_4$)] $^+\text{B}(\text{C}_6\text{F}_5)_4^-$ (6**). A 5 mm NMR tube fitted with a Teflon valve was charged with *ca.* 15 mg $(\text{dfepe})\text{Pt}(\text{Et})(\text{NC}_5\text{F}_5)^+\text{B}(\text{C}_6\text{F}_5)^-$ (**10**) and 0.3 mL *o*-difluorobenzene and cooled to $-20\text{ }^\circ\text{C}$. Approximately 5 equiv. ethylene was added via syringe and the solution was mixed well. The solution was warmed to $0\text{ }^\circ\text{C}$ and NMR data confirmed the clean formation of $[(\text{dfepe})\text{Pt}(\text{Et})(\eta^2\text{-C}_2\text{H}_4)]^+\text{B}(\text{C}_6\text{F}_5)_4^-$. ^1H NMR (400.13 MHz, *o*-difluorobenzene, acetone- d_6 external reference, $-50\text{ }^\circ\text{C}$; spectrum taken after $\sim 35\%$ conversion to **6**): δ 4.76 (s, br., $^2J_{\text{PtH}} = 55\text{ Hz}$, 4H; $\text{Pt}(\text{C}_2\text{H}_4)$), 1.96 (m, 2H; PCH_2), 1.65 (m, 2H; PCH_2), 1.41 (m, br., ($\nu_{1/2} \sim 40\text{ Hz}$), 2H; PtCH_2CH_3), -0.13 (m, br. ($\nu_{1/2} \sim 30\text{ Hz}$, 2H; PtCH_2CH_3). ^{31}P NMR (161.70 MHz, *o*-difluorobenzene, $0\text{ }^\circ\text{C}$): δ 73.8 (dm, $J_{\text{PP}} = 25\text{ Hz}$, $^1J_{\text{PtP}} = 1225\text{ Hz}$; P *trans* to Et), 62.8 (m, $^1J_{\text{PtP}} = 4740\text{ Hz}$, P *trans* to C_2H_4). ^{19}F NMR (376.5**

MHz, ODFB, -30 °C): δ -81.4 (s, 6F; PCF₂CF₃), -82.0 (s, 6F; PCF₂CF₃), -107 to -112 (overlapping ABX multiplets, 8F; PCF₂CF₃).

[(dfepe)Pt(¹³CH₃)(NC₅F₅)]⁺B(C₆F₅)₄⁻. (dfepe)Pt(¹³CH₃)₂ was prepared from the reaction of (dfepe)PtCl₂ with ¹³CH₃Li following a modified published procedure.¹⁸ To a flask charged with (dfepe)Pt(¹³CH₃)₂ (0.286 g, 0.361 mmol) and [Ph₃C]⁺B(C₆F₅)₄⁻ (0.346 g, 0.433 mmol) was added 15 mL of pentafluoropyridine. After stirring the mixture for 2 hrs the resulting white solid (0.452 g, 77 %) was collected by filtration and dried under vacuum. ¹H NMR (400.13 MHz, *o*-difluorobenzene, 27 °C): δ 2.02 (m, 2H; PCH₂), 1.72 (m, 2H; PCH₂), 0.18 (br. s, ²J_{PtH} = 43 Hz, ¹J_{CH} = 138 Hz, 3H; Pt(¹³CH₃)). ¹³C NMR (100.62 MHz, *o*-difluorobenzene, 27 °C): δ 1.90 (d, ¹J_{PtC} = 195 Hz, ¹J_{CH} = 138 Hz, ²J_{PC} = 75 Hz; Pt¹³CH₃).

[(dfepe)Pt(Me)(NC₅F₅)]⁺B(C₆F₅)₄⁻ Ethylene Dimerization Studies. In a typical experiment, 0.3 mL of *o*-difluorobenzene and [(dfepe)Pt(Me)(NC₅F₅)]⁺B(C₆F₅)₄⁻ (**1**) (13 mg, 0.0080 mmol) were placed in a 5 mm NMR tube fitted with a Teflon valve and an acetone-*d*₆ capillary and ethylene gas (10-238 equiv, based on integration relative to **1**) was added via gas-tight syringe at -20 °C. After thorough mixing, the tube was warmed to the desired temperature (-10 °C, 0 °C, 10 °C). Butenes production was evaluated by ¹H NMR based on integration of the methyl resonances of *cis*- and *trans*-2-butene (0.48 and 0.43 ppm, respectively).

(dmpe)PtMe₂ (13). (cod)PtMe₂ (0.500g, 1.50 mmol) and dmpe (0.400g, 1.51 mmol) were dissolved in 20 mL of benzene and the mixture was stirred overnight. The resulting white precipitate was collected, washed with hexanes and dried (yield: 0.522 g). The filtrate

was titrated with hexanes and yielded an additional 0.152 g product (total yield: 0.674 g, 92%). Anal. Calcd for $C_8H_{28}B_{10}P_2Pt$: C, 19.63%, H, 5.77%. Found: C, 19.69%, H, 5.26%. 1H NMR (benzene- d_6 , 400.13 MHz, 300 K): δ 3.50-1.50 (m, 10H; $C_2B_{10}H_{10}$), 1.06 (m, 12H; $P(CH_3)_2$), 0.92 (pseudo t, $J_{HP} \sim 14$ Hz, $^2J_{PtH} = 69$ Hz, 6H; $Pt(CH_3)_2$). ^{31}P NMR (benzene- d_6 , 161.967 MHz, 300 K): δ 55.9 (s, $^1J_{PtP} = 1730$ Hz).

(dppc)PtMe₂ (14) (cod)PtMe₂ (0.500g, 1.50 mmol) and dppc (0.770 g, 1.50 mmol) were dissolved in 20 mL of benzene and the mixture was stirred overnight. The resulting white precipitate was collected, washed with hexanes and dried (0.991 g, 89.5%). Anal. Calcd for $C_{28}H_{36}B_{10}P_2Pt$: C, 45.59%, H, 4.92%. Found: C, 45.74%, H, 4.51%. 1H NMR (benzene- d_6 , 400.13 MHz, 300 K): δ 8.17 (m, 8H; *o*- C_6H_5), 7.03 (m, 12H; *m,p*- C_6H_5), 2.6 (br. m ($\nu_{1/2} = 410$ Hz), 10H; $C_2B_{10}H_{10}$), 1.15 (pseudo t, $J_{HP} \sim 14$ Hz, $^2J_{PtH} = 71$ Hz, 6H; $Pt(CH_3)_2$). ^{31}P NMR (benzene- d_6 , 161.967 MHz, 300 K): δ 72.4 (s, $^1J_{PtP} = 1895$ Hz).

(dfppe)PtMe₂ (15). Compound **9** has been previously reported,¹⁸ and was prepared using a modified procedure: (cod)PtMe₂ (0.505 g, 1.52 mmol) and dfppe (1.150 g, 1.520 mmol) were dissolved in 20 mL benzene and the mixture was stirred overnight. The resulting white precipitate was collected, washed with hexanes and dried, giving 0.590 g. The filtrate was triturated with hexane to yield an additional 0.555 g, for a total of 1.145 g (90% overall yield). Anal. Calcd for $C_{28}H_{10}F_{20}P_2Pt$: C, 34.20%, H, 1.02%. Found: C, 34.40%, H, 1.06%.

[(dippe)PtMe(CO)]⁺B(C₆F₅)₄⁻ (17) A mixture of **8** (0.150 g, 0.308 mmol) and $[Ph_3C]^+B(C_6F_5)_4^-$ (0.284 g, 0.308 mmol) were dissolved in 25 mL *o*-difluorobenzene and frozen at -78 °C to prevent premature methyl abstraction. 1 atm of CO was added to the

flask and the mixture was warmed to ambient temperature and stirred overnight. After the volatiles were removed a yellow residue remained which was triturated in 25 mL diethyl ether for 30 minutes. Filtration yielded 0.300 g (83%) of yellow **11**. Anal. Calcd for $C_{40}H_{35}F_{20}OP_2Pt$: C, 41.11%, H, 3.02%. Found C, 41.24%, H, 3.28%. 1H NMR (acetone- d_6 , 400.13 Hz, 300 K): δ 2.87 (m, 2H; $PCH(CH_3)_2$), 2.76 (m, 2H; $PCH(CH_3)_2$), 2.47 (m, 4H; PCH_2), 1.33 (m, 24H; $PCH(CH_3)_2$), 1.06 (virtual t, $^3J_{PH} = 6$ Hz, $^2J_{PtH} = 59$ Hz, 3H; $PtCH_3$). ^{31}P NMR (acetone- d_6 , 161.967 MHz, 300K): δ 88.2 (s, $^1J_{PtP} = 1590$ Hz; P trans to Pt-Me), 71.8 (s, $^1J_{PtP} = 3020$ Hz; P trans to Pt(CO)). IR (CH_2Cl_2): $\nu(CO) = 2106$ cm^{-1} .

[(dppp)PtMe(CO)] $^+$ B(C₆F₅)₄ $^-$ (20) A mixture of **11** (0.205g, 0.322 mmol) and $Ph_3C^+B(C_6F_5)_4^-$ (0.297g, 0.322 mmol) were dissolved in 25 mL *o*-difluorobenzene and frozen at -78 °C to prevent premature methyl abstraction. 1 atm of CO was added to the flask and the mixture was warmed to ambient temperature and stirred overnight. Volatiles were removed and the residue was triturated in petroleum ether; the isolated yield of **20** after filtration and drying was 0.200 g (49%). Anal. Calcd for $C_{53}H_{29}BF_{20}OP_2Pt$: C, 47.88%, H, 2.20%. Found C, 48.16%, H, 2.85%. 1H NMR (acetone- d_6 , 400.13 Hz, 300 K): δ 7.8-7.5 (m, 20H; $2P(C_6H_5)_2$), 3.18 (m, 4H; CH_2P), 2.27 (m, 2H; $PCH_2CH_2CH_2P$), 0.69 (virtual t, $J_{PH} = 6$ Hz, $^2J_{PtH} = 58$ Hz, 3H; $Pt-CH_3$). ^{31}P NMR (acetone- d_6 , 161.967 MHz, 300 K): δ 2.3 (d, $J_{PP} = 35$ Hz, $^1J_{PtP} = 3125$ Hz; P trans to Pt(CO)), -5.5 (d, $J_{PP} = 35$ Hz, $^1J_{PtP} = 1580$ Hz; P trans to PtCH₃). IR (CH_2Cl_2): $\nu(CO) = 2117$ cm^{-1} .

[(dppb)PtMe(CO)] $^+$ B(C₆F₅)₄ $^-$ (21) A mixture of **12** (0.204 g, 0.313 mmol) and $Ph_3C^+B(C_6F_5)_4^-$ (0.289 g, 0.313 mmol) were dissolved in 25 mL *o*-difluorobenzene and frozen at -78 °C to prevent premature methyl abstraction. 1 atm of CO was added to the

flask and the mixture was warmed to ambient temperature and stirred overnight. ODF was pulled off by dynamic vacuum. Volatiles were removed and the residue was triturated in petroleum ether; the isolated yield of **21** after filtration and drying was 0.260 g (62%). Anal. Calcd for $C_{54}H_{31}BF_{20}OP_2Pt$: C, 48.27%, H, 2.33%. Found C, 48.80%, H, 3.19%. 1H NMR (acetone- d_6 , 400.13 Hz, 300 K): δ 7.9 - 7.4 (m, 20H; $2P(C_6H_5)_2$), 3.28 (m, 2H; CH_2P), 3.03 (m, 2H; CH_2P), 2.20 (m, 2H, CH_2CH_2P), 1.79 (m, 2H, CH_2CH_2P), 0.83 (virtual t, $J_{PH} = 6$ Hz, $^2J_{PtH} = 58$ Hz, 3H; Pt- CH_3). ^{31}P NMR (acetone- d_6 , 161.967 MHz, 300 K): δ 15.4 (d, $^2J_{PP} = 27$ Hz, $^1J_{PtP} = 3230$ Hz; P trans to Pt(CO)), 14.2 (d, $^2J_{PP} = 27$ Hz, $^1J_{PtP} = 1700$ Hz; P trans to PtMe). IR (CH_2Cl_2): $\nu(CO) = 2118$ cm^{-1} .

[(dmpc)PtMe(CO)] $^+$ B(C $_6$ F $_5$) $_4^-$ (22) A mixture of **13** (0.205 g, 0.419 mmol) and $[Ph_3C]^+B(C_6F_5)_4^-$ (0.377 g, 0.409 mmol) were dissolved in 25 mL *o*-difluorobenzene and frozen at -78 °C to prevent premature methyl abstraction. 1 atm of CO was added to the flask and the mixture was warmed to ambient temperature and stirred overnight. After the volatiles were removed a yellow solid residue remained which was triturated in 25 mL diethyl ether for 30 minutes. The resulting white powder was filtered, washed with ether, and dried to give 0.344 g (75%) of **22**. Anal. Calcd for $C_{32}H_{25}B_{11}F_{20}OP_2Pt$: C, 32.53%, H 2.13%. Found: C, 33.22%, H, 2.32%. 1H NMR (acetone- d_6 , 400.13 MHz, 300 K): δ 3.4 - 1.6 (br. m ($\nu_{1/2} = 500$ Hz), 10H; $C_2B_{10}H_{10}$), 2.42 (d, $^2J_{PH} = 10$ Hz, $^3J_{PtH} = 18$ Hz, 6H; $P(CH_3)_2$ trans to Pt-Me), 2.26 (d, $^2J_{PH} = 11$ Hz, $^3J_{PtH} = 42$ Hz, 6H; $P(CH_3)_2$ trans to Pt-CO), 1.00 (virtual t, $^3J_{PH} = 7$ Hz, $^2J_{PtH} = 57$ Hz, 3H; Pt- CH_3). ^{31}P NMR (acetone- d_6 , 161.967 MHz, 300 K): δ 49.6 (d, $J_{PP} = 24$ Hz, $^1J_{PtP} = 3250$ Hz; P trans to Pt-CO), 60.5 (d, $J_{PP} = 24$ Hz, $^1J_{PtP} = 1680$ Hz; P trans to Pt-Me). IR (CH_2Cl_2): $\nu(CO) = 2132$ cm^{-1} .

Spectroscopy for [(dmpe)PtMe(CO)]⁺B(C₆F₅)₄⁻ (16), [(dppm)PtMe(CO)]⁺SbF₆⁻ (18), [(dppe)PtMe(CO)]⁺B(C₆F₅)₄⁻ (19), [(dppc)PtMe(CO)]⁺B(C₆F₅)₄⁻ (23), and [(dfppe)PtMe(CO)]⁺B(C₆F₅)₄⁻(24): Following an analogous synthetic procedure employed for the other (PP)Pt(Me)(CO)⁺ compounds in this study, [(dmpe)PtMe(CO)]⁺B(C₆F₅)₄⁻ and [(dfppe)PtMe(CO)]⁺B(C₆F₅)₄⁻ were not isolated as pure materials, but were characterized by NMR and IR. Treatment of (dppm)PtMe₂ with [Ph₃C]⁺SbF₆⁻ under 1 atm CO in DFB gave [(dppm)PtMe(CO)]⁺SbF₆⁻ as a minor (~ 40%) initially formed product which was partially characterized by IR and ³¹P NMR.

[(dmpe)PtMe(CO)]⁺B(C₆F₅)₄⁻ (16): ¹H NMR (acetone-*d*₆, 400.13 Hz, 300 K): δ 2.44 (m, 4H; CH₂P), 2.03 (d, ²J_{PH} = 11 Hz, ³J_{PTH} = 10 Hz, 6H; P(CH₃)), 1.85 (d, ²J_{PH} = 12 Hz, ³J_{PTH} = 10 Hz, 6H; P(CH₃)), 0.86 (virtual t, J_{PH} = 6 Hz, ²J_{PTH} = 59 Hz, 3H; PtCH₃). ³¹P NMR (acetone-*d*₆, 161.967 MHz, 300 K): δ 38.2 (d, J_{PP} = 8 Hz, ¹J_{PtP} = 1580 Hz; P trans to PtMe), 34.0 (d, J_{PP} = 8 Hz, ¹J_{PtP} = 2985 Hz; P trans to Pt(CO)). IR (CH₂Cl₂): ν(CO) = 2112 cm⁻¹.

[(dppm)PtMe(CO)]⁺SbF₆⁻ (18): ³¹P NMR (*o*-difluorobenzene, 161.967 MHz, 300 K): δ -31.4 (d, ²J_{PP} = 50 Hz), -40.3 (d, ²J_{PP} = 50 Hz). IR (CH₂Cl₂): ν(CO) = 2110 cm⁻¹.

[(dppe)PtMe(CO)]⁺B(C₆F₅)₄⁻ (19): ¹H NMR (acetone-*d*₆, 400.13 Hz, 300 K): δ 7.9 - 7.1 (m, 20H; P(C₆H₅)₂), 3.05 (m, 4H; CH₂P), 0.99 (virtual t, ³J_{PH} = 6 Hz, ²J_{PTH} = 61 Hz, 3H; PtCH₃). ³¹P NMR (acetone-*d*₆, 161.967 MHz, 300 K): δ 53.4 (d, J_{PP} = 8 Hz, ¹J_{PtP} = 1620 Hz; P trans to PtCH₃), 50.3 (d, J_{PP} = 8 Hz, ¹J_{PtP} = 3190 Hz; P trans to Pt(CO)). IR (CH₂Cl₂): ν(CO) = 2114 cm⁻¹.

[(dppc)PtMe(CO)]⁺B(C₆F₅)₄⁻ (23): ¹H NMR (acetone-*d*₆, 400.13 MHz, 300 K): δ 8.49 (dd, ³J_{PH} = 14 Hz, ³J_{HH} = 7 Hz, 4H; *o*-C₆H₅), 8.39 (dd, ³J_{PH} = 14 Hz, ³J_{HH} = 7 Hz, 4H; *o*-C₆H₅), 7.86 (overlapping m, 12H; *m,p*-C₆H₅), 2.3 (br m (*v*_{1/2} = 400 Hz), 10H; C₂B₁₀H₁₀), 1.05 (virtual t, ³J_{PH} = 6 Hz, ²J_{PtH} = 58 Hz, 3H; Pt-CH₃). ³¹P NMR (acetone-*d*₆, 161.967 MHz, 300 K): δ 61.8 (d, J_{PP} = 24 Hz, ¹J_{PtP} = 1775 Hz; P trans to Pt-Me), 61.2 (d, J_{PP} = 24 Hz, ¹J_{PtP} = 3563 Hz; P trans to Pt(CO)). IR (CH₂Cl₂): ν(CO) = 2133 cm⁻¹.

[(dfppe)PtMe(CO)]⁺B(C₆F₅)₄⁻ (24): ¹H NMR (acetone-*d*₆, 400.13 Hz, 300 K): δ 3.66 (m, 4H; CH₂P), 1.17 (br., virtual t, J_{PH} = 8 Hz, ²J_{PtH} = 61 Hz, 3H; PtCH₃). ³¹P NMR (acetone-*d*₆, 161.967 MHz, 300 K): δ 18.9 (s, ¹J_{PtP} = 1395 Hz; P trans to PtMe), 18.1 (s, ¹J_{PtP} = 3560 Hz; P trans to Pt(CO)). IR (CH₂Cl₂): ν(CO) = 2149 cm⁻¹

NMR characterization of (PP)Pt(Me)(C₂H₄)⁺ and (PP)Pt(Et)(C₂H₄)⁺ complexes.

Treatment of (PP)PtMe₂ with Ph₃C⁺B(C₆F₅)₄⁻ in *o*-difluorobenzene in the presence of excess ethylene results in the clean formation of (PP)Pt(Me)(C₂H₄)⁺ adducts with sufficient stability (several hours) to allow characterization by ¹H and ³¹P NMR. In most cases clean conversion to (PP)Pt(Et)(C₂H₄)⁺ occurred during the course of catalytic runs, as judged by ³¹P NMR.

(dmpe)PtMe(C₂H₄)⁺ (25): ¹H NMR (*o*-difluorobenzene, 400.13 MHz, 300 K): Pt(C₂H₄) obscured by free ethylene resonance at 4.29 ppm; δ 0.66 (m, 4H; PCH₂), 0.35 (m, 12H; overlapping P(CH₃), -0.50 (virtual t, ³J_{PH} = 6 Hz, ²J_{PtH} = 50 Hz, 3H; Pt(CH₃)). ³¹P NMR (*o*-difluorobenzene, 161.967 MHz, 300 K): δ 36.9 (s, ¹J_{PtP} = 3460 Hz; P trans to Pt(C₂H₄)), 32.5 (d, ¹J_{PtP} = 1635 Hz; P trans to PtMe).

(dippe)PtMe(C₂H₄)⁺ (26): ¹H NMR (*o*-difluorobenzene, 400.13 MHz, 300 K): δ 4.05 (br. s, ²J_{PtH} = 44 Hz, 4H; Pt(C₂H₄)), 1.43 (doublet of septets, ³J_{HH} = 7.5 Hz, ²J_{PH} = 9 Hz, 2H; P(CH(CH₃)₂)₂), 1.30 (doublet of septets, ³J_{HH} = ²J_{PH} = 8 Hz, 2H; P(CH(CH₃)₂)₂), 0.89 (m, 2H; PCH₂), 0.73 (m, 2H; PCH₂), 0.08 (m, 24H; overlapping P(CH(CH₃)₂)₂), -0.37 (dd, ³J_{PH} = 3.5, 6 Hz, ²J_{PtH} = 49 Hz, 3H; Pt(CH₃)). ³¹P NMR (*o*-difluorobenzene, 161.967 MHz, 300 K): δ 72.8 (s, ¹J_{PtP} = 3805 Hz; P trans to Pt(C₂H₄)), 71.8 (d, ¹J_{PtP} = 1670 Hz; P trans to PtMe).

(dppm)PtMe(C₂H₄)⁺ (27): ¹H NMR (*o*-difluorobenzene, 400.13 MHz, 300 K): δ 6.6 – 6.0 (dppm aryl resonances, obscured by solvent), 3.73 (virtual t, ²J_{PH} = 11 Hz, ²J_{PtH} = 50 Hz, 2H; P(CH₂)P), 0.14 (m, ²J_{PtH} = 60 Hz, 3H; PtCH₃). ³¹P NMR (*o*-difluorobenzene, 161.967 MHz, 300 K): δ -36.8 (d, J_{PP} = 67 Hz, ¹J_{PtP} = 4360 Hz; P trans to Pt(C₂H₄)), -44.4 (d, J_{PP} = 67 Hz, ¹J_{PtP} = 1290 Hz; P trans to PtMe).

(dppe)PtMe(C₂H₄)⁺ (28): ¹H NMR (*o*-difluorobenzene, 400.13 MHz, 300 K): δ 6.8 – 6.5 (m, 20H; overlapping PPh), 1.52 (m, 4H; PCH₂), -0.07 (virtual t, ²J_{PH} = 5 Hz, ²J_{PtH} = 52 Hz, 3H; PtCH₃). ³¹P NMR (*o*-difluorobenzene, 161.967 MHz, 300 K): δ 54.2 (d, J_{PP} = 8 Hz, ¹J_{PtP} = 1670 Hz; P trans to PtMe), 52.7 (d, J_{PP} = 8 Hz, ¹J_{PtP} = 3830 Hz; P trans to Pt(C₂H₄)).

(dppp)PtMe(C₂H₄)⁺ (29): ¹H NMR (*o*-difluorobenzene, 400.13 MHz, 300 K): δ 6.6 – 6.3 (m, 20H; overlapping dppp aryl resonances), 1.63 (m, 4H; PCH₂), 0.99 (m, 2H; PCH₂CH₂), -0.49 (m, ²J_{PtH} = 50 Hz, 3H; PtCH₃). ³¹P NMR (*o*-difluorobenzene, 161.967 MHz, 300 K): δ 4.8 (d, J_{PP} = 8 Hz, ¹J_{PtP} = 1550 Hz; P trans to PtMe), 4.5 (d, J_{PP} = 27 Hz, ¹J_{PtP} = 3920 Hz; P trans to Pt(C₂H₄)).

(dppb)PtMe(C₂H₄)⁺ (30): ¹H NMR (*o*-difluorobenzene, 400.13 MHz, 300 K): δ 6.4 (m, 20H; overlapping dppb aryl resonances), 1.75 (m, 2H; PCH₂), 1.56 (m, 2H; PCH₂), 1.05 (m, 2H; PCH₂CH₂), 0.50 (m, 2H; PCH₂CH₂), -0.43 (virtual t, ²J_{PH} = 6 Hz, ²J_{PtH} = 49 Hz, 3H; PtCH₃). ³¹P NMR (*o*-difluorobenzene, 161.967 MHz, 300 K): δ 25.9 (d, J_{PP} = 19 Hz, ¹J_{PtP} = 1690 Hz; P trans to PtMe), 11.7 (d, J_{PP} = 19 Hz, ¹J_{PtP} = 3980 Hz; P trans to Pt(C₂H₄)).

(dmPC)PtMe(C₂H₄)⁺ (31): ¹H NMR (*o*-difluorobenzene, 400.13 MHz, 300 K): δ 3.50-1.50 (br. m (v_{1/2} = 500 Hz), 10H; C₂B₁₀H₁₀), 0.82 (d, ²J_{PH} = 11 Hz, ³J_{PtH} = 48 Hz, 6H; P(CH₃)₂ trans to Pt(C₂H₄)), 0.74 (d, ²J_{PH} = 8 Hz, ³J_{PtH} = 14 Hz, 6H; P(CH₃)₂ trans to PtMe), -0.50 (virtual t, ³J_{PH} = 6 Hz, ²J_{PtH} = 47 Hz, 3H; PtCH₃). ³¹P NMR (*o*-difluorobenzene, 161.967 MHz, 300 K): δ 55.7 (d, J_{PP} = 18 Hz, ¹J_{PtP} = 1670 Hz; P trans to PtMe), 49.7 (d, J_{PP} = 18 Hz, ¹J_{PtP} = 3980 Hz; P trans to Pt(C₂H₄)).

(dppc)PtMe(C₂H₄)⁺ (32): ¹H NMR (*o*-difluorobenzene, 400.13 MHz, 300 K): δ 7.04 (dd, ³J_{PH} = 13 Hz, ³J_{HH} = 8 Hz, 4H; *o*-C₆H₅), 6.88 (ddm, ³J_{PH} = 12 Hz, ³J_{HH} = 8 Hz, 4H; *o*-C₆H₅), 6.55 (overlapping m, 12H; *m,p*-C₆H₅), 3.95 (br. s, ²J_{PtH} = 48 Hz, 4H; Pt(C₂H₄)), 1.3 (br m (v_{1/2} = 300 Hz), 10H; C₂B₁₀H₁₀), -0.35 (virtual t, ³J_{PH} = 6 Hz, ²J_{PtH} = 48 Hz, 3H; Pt-CH₃). ³¹P NMR (*o*-difluorobenzene, 161.967 MHz, 300 K): δ 67.5 (d, J_{PP} = 18 Hz, ¹J_{PtP} = 1730 Hz; P trans to PtMe), 63.0 (d, J_{PP} = 18 Hz, ¹J_{PtP} = 4330 Hz; P trans to Pt(C₂H₄)).

(dfppe)PtMe(C₂H₄)⁺ (33): ¹H NMR (*o*-difluorobenzene, 400.13 MHz, 300 K): δ 2.18 (m, 4H; PCH₂), -0.08 (m, ²J_{PtH} = 52 Hz, 3H; PtCH₃). ³¹P NMR (*o*-difluorobenzene, 161.967 MHz, 300 K): δ 22.9 (d, J_{PP} = 10 Hz, ¹J_{PtP} = 1565 Hz; P trans to Pt(Me)), 15.6 (d, J_{PP} = 10 Hz, ¹J_{PtP} = 4370 Hz; P trans to Pt(C₂H₄)).

(dippe)PtEt(C₂H₄)⁺: ³¹P NMR (*o*-difluorobenzene, 161.967 MHz, 300 K): δ 72.1 (s, ¹J_{PtP} = 3930 Hz; P trans to Pt(C₂H₄)), 71.2 (s, ¹J_{PtP} = 1530 Hz; P trans to Pt(Et)).

(dppm)Pt(Et)(C₂H₄)⁺: ³¹P NMR (*o*-difluorobenzene, 161.967 MHz, 300 K): dilute, ¹⁹⁵Pt satellites not observed, δ -34.0 (d, J_{PP} = 66 Hz), -41.7 (d, J_{PP} = 66 Hz).

(dppe)Pt(Et)(C₂H₄)⁺: ³¹P NMR (*o*-difluorobenzene, 161.967 MHz, 300 K): δ 53.6 (d, J_{PP} = 9 Hz, ¹J_{PtP} = 3990 Hz; P trans to Pt(C₂H₄)), 51.1 (d, J_{PP} = 9 Hz, ¹J_{PtP} = 1530 Hz; P trans to Pt(Me)).

(dppp)Pt(Et)(C₂H₄)⁺: ³¹P NMR (*o*-difluorobenzene, 161.967 MHz, 300 K): δ 5.6 (d, J_{PP} = 28 Hz, ¹J_{PtP} = 4130 Hz; P trans to Pt(C₂H₄)), 4.5 (d, J_{PP} = 28 Hz, ¹J_{PtP} = 1400 Hz; P trans to Pt(Et)).

(dppb)Pt(Et)(C₂H₄)⁺: ³¹P NMR (*o*-difluorobenzene, 161.967 MHz, 300 K): δ 26.6 (d, J_{PP} = 18 Hz, ¹J_{PtP} = 1535 Hz; P trans to Pt(Et)), 13.8 (d, J_{PP} = 18 Hz, ¹J_{PtP} = 4220 Hz; P trans to Pt(C₂H₄)).

(dmpe)PtEt(C₂H₄)⁺: ³¹P NMR (*o*-difluorobenzene, 161.967 MHz, 300 K): δ 54.3 (d, J_{PP} = 21 Hz, ¹J_{PtP} = 1520 Hz; P trans to PtMe), 49.4 (d, J_{PP} = 21 Hz, ¹J_{PtP} = 4140 Hz; P trans to Pt(C₂H₄)).

(dppc)PtEt(C₂H₄)⁺: ³¹P NMR (*o*-difluorobenzene, 161.967 MHz, 300 K): δ 68.1 (d, J_{PP} = 20 Hz, ¹J_{PtP} = 1600 Hz; P trans to PtMe), 63.8 (d, J_{PP} = 20 Hz, ¹J_{PtP} = 4505 Hz; P trans to Pt(C₂H₄)).

(dfppe)PtEt(C₂H₄)⁺: ³¹P NMR (*o*-difluorobenzene, 161.967 MHz, 300 K): δ 21.1 (s, ¹J_{PtP} = 1395 Hz; P trans to Pt(Et)), 17.1 (s, ¹J_{PtP} = 4650 Hz; P trans to Pt(C₂H₄)).

Partial characterization of (PP)Pt(η^3 -C₃H₄Me)⁺ products: Ethylene dimerization catalyst studies with (dippe)PtEt₂, (dppb)PtEt₂, and (dmcp)PtEt₂ (see above) generated, after complete ethylene consumption, products tentatively identified as methylallyl cationic complexes on the basis of partial NMR characterization and the structural characterization of [(dmcp)Pt(η^3 -C₃H₄Me)]⁺B(C₆F₅)₄⁻ (**34**) and [(dfepe)Pt(η^3 -C₃H₄Me)]⁺B(C₆F₅)₄⁻ (**35**). **NMR data for (dppb)Pt(η^3 -C₃H₄Me)⁺:** ³¹P NMR (*o*-difluorobenzene, 161.967 MHz, 300 K): δ 4.6 (br. s, ¹J_{PtP} = 3530 Hz). ¹H NMR (*o*-difluorobenzene, 400.13 MHz, 300 K): δ 0.32 (s; Pt(η^3 -C₃H₄CH₃)). **NMR data for (dippe)Pt(η^3 -C₃H₄Me)⁺:** ³¹P NMR (*o*-difluorobenzene, 161.967 MHz, 300 K): δ 66.0 (br. s, ¹J_{PtP} = 3520 Hz). ¹H NMR (*o*-difluorobenzene, 400.13 MHz, 300 K): δ -0.24 (s; Pt(η^3 -C₃H₄CH₃)). **NMR data for (dmcp)Pt(η^3 -C₃H₄Me)⁺:** ³¹P NMR (*o*-difluorobenzene, 161.967 MHz, 300 K): δ 47.3 (AB spin system, δ_A = 47.35, ¹J_{PtP_A} = 3732 Hz, δ_B = 47.20, ¹J_{PtP_B} = 3722 Hz, J_{PP} = 15.5 Hz).

Determination of ethylene dimerization catalytic activities. In a typical experiment, a Teflon-valved 5 mm NMR tube containing a sealed acetone-*d*₆ capillary was charged with 10 mg of catalyst and 0.5 mL *o*-difluorobenzene, and excess ethylene was condensed in at 77 K. Integration of initial ¹H NMR spectra quantified the initial amount of added ethylene, which was typically ~ 25 equivalents. ¹H NMR spectra at 22 °C were taken at intervals using both the residual acetone-*d*₅ and the *o*-difluorobenzene as reference standards. Integration of *cis*- and *trans*-2-butene product methyl resonances was used to

determine TOF and TON values; Pt-Me insertion rates were determined by disappearance of Pt-Me resonances using acetone- d_5 as an internal standard.

X-Ray Crystallography. X-ray diffraction data for **2**, **17**, **34** and **35** were measured at 150 K on a Bruker SMART APEX II CCD area detector system equipped with a graphite monochromator and a Mo $K\alpha$ fine-focus sealed tube operated at 1.5 kW power (50 kV, 30 mA). Crystals were attached to glass fibers using Paratone N oil. Collection and refinement details are included in the supplementary material. Crystallographic data (excluding structure factors) for the structures reported in this paper were deposited with the Cambridge Crystallographic Data Centre (see below).

Computational Details. All calculations were carried out using Gaussian 09 Rev. A.02,²⁹ using the M06-L functional for geometry optimization and frequencies.³⁰ A def2-QZVP basis set was used for platinum and def2-TZVP basis sets were used for the remaining atoms.³¹ An ECP basis set for def2 bases was used.³² Converged transition state geometries were confirmed by observing single negative vibration modes along the insertion coordinate. NBO analysis (version 3) and accompanying Mayer bond order indices are implemented in Gaussian 09.

Acknowledgements: We thank The National Science Foundation (CHE-1566622) for financial support.

Appendix A. Supplementary Data

Synthesis of $^{13}\text{CH}_3\text{Li}$, representative NMR spectra, X-ray diffraction refinement details for **2**, **17**, **34**, and **35**, and selected kinetic plots. X-ray data for CCDC-1975348 (**2**), 1974629

([17](#)), 1974627 ([34](#)) and 1974628 ([35](#)) can be obtained free of charge via <http://www.ccdc.cam.ac.uk/conts/retrieving.html>, or from the Cambridge Crystallographic Data Centre, 12 Union Road, Cambridge CB2 1EZ, UK; fax: +44 1223 336 033; or e-mail: deposit@ccdc.cam.ac.uk.

References

1. (a) Eisch, J. J., "Fifty Years of Ziegler-Natta Polymerization: From Serendipity to Science. A Personal Account" *Organometallics* **2012**, *31*, 4917-4932; (b) McDaniel, M. P., in *Review of Phillips chromium catalyst for ethylene polymerization*, John Wiley & Sons, Inc.: 2010; pp 291-446; (c) Mulhaupt, R., "Catalytic polymerization and post polymerization catalysis fifty years after the discovery of Ziegler's catalysts" *Macromol. Chem. Phys.* **2003**, *204* (2), 289-327; (d) Bohm, L. L., "The ethylene polymerization with Ziegler catalysts: fifty years after the discovery" *Angew. Chem. Int. Ed., Eng.* **2003**, *42*, 5010-5030; (e) Clark, A.; Hogan, J. P.; Banks, R. L.; Lanning, W. C., "Marlex catalyst systems" *Ind. Eng. Chem.* **1956**, *48*, 1152-1155; (f) Ziegler, K.; Holzkamp, E.; Breil, H.; Martin, H., "Aluminum in organic chemistry. VII. Polymerization of ethylene and other olefins" *Angewandte Chemie* **1955**, *67*, 426.
2. (a) Keim, W., "Oligomerization of ethylene to α -olefins: discovery and development of the shell higher olefin process (SHOP)" *Angew. Chem. Int. Ed.*, **2013**, *52*, 12492-12496; (b) Skupinska, J., "Oligomerization of α -olefins to higher oligomers" *Chem. Rev.* **1991**, *91*, 613-648.
3. Ittel, S. D.; Johnson, L. K.; Brookhart, M., "Late-Metal Catalysts for Ethylene Homo- and Copolymerization" *Chem. Rev.* **2000**, *100*, 1169-1203.
4. Johnson, L. K.; Killian, C. M.; Brookhart, M., "New Pd(II)- and Ni(II)-Based Catalysts for Polymerization of Ethylene and α -Olefins. *J. Am. Chem. Soc.* **1995**, *117*, 6414-6415.

5. (a) Mecking, S.; Johnson, L. K.; Wang, L.; Brookhart, M., "Mechanistic Studies of the Palladium-Catalyzed Copolymerization of Ethylene and α -Olefins with Methyl Acrylate" *J. Am. Chem. Soc.* **1998**, *120*, 888-899; (b) Killian, C. M.; Tempel, D. J.; Johnson, L. K.; Brookhart, M., Living polymerization of α -olefins using Ni(II)- α -diimine catalysts. Synthesis of new block polymers based on α -olefins" *J. Am. Chem. Soc.* **1996**, *118*, 11664-11665.
6. Shiotsuki, M.; White, P. S.; Brookhart, M.; Templeton, J. L., "Mechanistic Studies of Platinum(II)-Catalyzed Ethylene Dimerization: Determination of Barriers to Migratory Insertion in Diimine Pt(II) Hydrido Ethylene and Ethyl Ethylene Intermediates" *J. Am. Chem. Soc.* **2007**, *129*, 4058-4067.
7. White, S.; Bennett, B. L.; Roddick, D. M., "Organometallics in Acidic Media: Catalytic Dimerization of Ethylene by (Perfluoroalkyl)phosphine Complexes of Platinum and Palladium in Trifluoroacetic Acid" *Organometallics* **1999**, *18*, 2536-2542.
8. Basu, S.; Arulsamy, N.; Roddick, D. M., "Synthesis of [(dfepe)Pt(Me)(NC₅F₅)⁺B(C₆F₅)₄⁻], a Highly Active Ethylene Dimerization Catalyst" *Organometallics* **2008**, *27*, 3659-3665.
9. The temperature and activity that we initially reported⁸ were incorrect. These are the correct values.
10. (a) Visalakshi, R.; Patel, R. P., Synthesis and characterization of palladium(II) chloride and platinum(II) chloride complexes with substituted anilines. *Synth. React. Inorg. Met.-Org. Chem.* **1994**, *24*, 1043-1053; (b) Pavlenko, N. I.; Aksyutina, L. A.; Rubailo, A. I., "IR-spectroscopic study of chloride complexes of platinum(II) and palladium(II) with perfluorinated aromatic amines" *Koord. Khim.* **1982**, *8*, 205-210.
11. (a) Vicente, J.; Chicote, M. T.; Beswick, M. A.; de Arellano, M. C. R., "Platinum-Assisted Addition of Carbonyl-Stabilized Phosphorus Ylides to Pentafluorobenzonitrile and Acetonitrile To Give Platinum(II) Complexes Containing Iminophosphorane and/or N-Bonded β -Imino Phosphorus Ylide

- Ligands. Crystal and Molecular Structures of *trans*-[PtCl₂{E-NH=C(C₆F₅)C(=PPh₃)C(O)Me}₂] and *trans*-[PtCl₂{E-N(=PPh₃)C(C₆F₅)=CHCO₂Et}{E-NH=C(C₆F₅)C(=PPh₃)CO₂Et}]” *Inorg. Chem.* **1996**, *35*, 6592-6598; (b) Goel, R. G.; Srivastava, R. C., “Preparation, characterization, and some reactions of hydridobis(tri-tert-butyl)phosphineplatinum(II) cation containing three-coordinate platinum” *Can. J. Chem.* **1983**, *61*, 1352-1359; (c) Chisholm, M. H.; Clark, H. C.; Manzer, L. E.; Stothers, J. B.; Ward, J. E. H., “Carbon-13 nuclear magnetic resonance studies. 35. Carbon-13 nuclear magnetic resonance studies of organometallic compounds. I. *trans*-Methylplatinum(II) derivatives” *J. Am. Chem. Soc.* **1973**, *95*, 8574; (d) Clark, H. C.; Manzer, L. E., “Cationic organometallic complexes with unsaturated systems. I. Methylplatinum(II)-nitrile and -imino ether complexes” *Inorg. Chem.* **1971**, *10*, 2699-2704; (e) Chisholm, M. H.; Clark, H. C.; Manzer, L. E.; Stothers, J. B., “Relations between carbon-13 nuclear magnetic resonance parameters, *trans*-influences, and ligand reactivities for methylplatinum compounds” *J. Chem. Soc. D.* **1971**, 1627-1629.
12. A higher coalescence point for (dfep)Pt(Et)(C₂H₄)⁺ (above -10 °C) relative to (dfep)Pt(Et)(NC₅F₅)⁺ is expected due to stronger ethylene binding relative to pentafluoropyridine, as indicated by 1J_{PtP} values (4370 Hz and 4950 Hz, respectively)
 13. McBee, J. L.; Bell, A. T.; Tilley, T. D., “Mechanistic Studies of the Hydroamination of Norbornene with Electrophilic Platinum Complexes: The Role of Proton Transfer” *J. Am. Chem. Soc.* **2008**, *130*, 16562-16571.
 14. Togo, Y.; Kanazawa, A.; Kanaoka, S.; Aoshima, S., “Controlled Cationic Polymerization of 1-Methoxy-1,3-Butadiene: Long-Lived Species-Mediated Reaction and Control over Microstructure with Weak Lewis Bases” *J. Polym. Sci., Part A: Polym. Chem.* **2019**, *57*, 288-296.
 15. Brown, H. C.; Kanner, B., “Preparation and reactions of 2,6-di-tert-butylpyridine and related hindered bases. A case of steric hindrance toward the proton” *J. Am. Chem. Soc.* **1966**, *88*, 986-992.

16. Parson, T. G.; Butikofer, J. L.; Houllis, J. F.; Roddick, D. M., "Organometallics in Superacidic Media: Characterization of Remarkably Stable Platinum-Methyl Bonds in HF/SbF₅ Solution" *Organometallics* **2017**, *36*, 136-141.
17. (a) Romeo, R.; D'Amico, G., "Mechanistic Insight into the Protonolysis of the Pt-C Bond as a Model for C-H Bond Activation by Platinum(II) Complexes" *Organometallics* **2006**, *25*, 3435-3446; (b) Schwartz, D. J.; Ball, G. E.; Andersen, R. A., "Interactions of cis-P₂PtX₂ Complexes (X = H, Me) with Bis(pentamethylcyclopentadienyl)ytterbium" *J. Am. Chem. Soc.* **1995**, *117*, 6027-6040; (c) Hietkamp, S.; Stufkens, D. J.; Vrieze, K., "Ring size effects on some carbon-13, phosphorus-31 and platinum-195 NMR parameters in the series {Ph₂P(CH₂)_nPh₂}Pt(CH₃)₂" *J. Organomet. Chem.* **1979**, *169*, 107-113; (d) Appleton, T. G.; Bennett, M. A.; Tomkins, I. B., "Effect of chelate-ring size on spectroscopic and chemical properties of methylplatinum(II) complexes of the ditertiary phosphines phosphines Ph₂P[CH₂]_nPPh₂ (n = 1,2 or 3). *J. Chem. Soc., Dalton Trans.* **1976**, 439-446.
18. Merwin, R. K.; Schnabel, R. C.; Koola, J. D.; Roddick, D. M., "Kinetics and mechanism of biaryl reductive elimination from electron-poor platinum complexes [(C₆F₅)₂PCH₂CH₂P(C₆F₅)₂]Pt(Ar)₂" *Organometallics* **1992**, *11*, 2972-2978.
19. Chien, J. C. W.; Tsai, W. M.; Rausch, M. D., "Isospecific polymerization of propylene catalyzed by rac-ethylenebis(indenyl)methylzirconium cation" *J. Am. Chem. Soc.* **1991**, *113*, 8570-8571.
20. Hutton, A. T.; Shabanzadeh, B.; Shaw, B. L., [Pt₂Me₂(μ-Ph₂PCH₂PPh₂)₂][BF₄]₂, a highly reactive and coordinatively unsaturated diplatinum(II) complex. Crystal structures of [Pt₂Me₂L₂(μ-Ph₂PCH₂PPh₂)₂][BF₄]₂ (L = acetonitrile or carbon monoxide). *J. Chem. Soc., Chem. Commun.* **1983**, 1053-1055.
21. Houllis, J. F.; Roddick, D. M., "Organometallics in Superacidic Media: Generation of Highly Electrophilic (Fluoroalkyl)phosphine Pt(II) Cationic Complexes" *J. Am. Chem. Soc.* **1998**, *120*, 11020-11021.

22. Mayer, I., "Bond order and valence indices: A personal account" *J. Comp. Chem.* **2007**, *28*, 204-221.
23. (a) Costa, E.; Pringle, P. G.; Ravetz, M., "[(1,2,5,6- η)-1,5-Cyclooctadiene]dimethylplatinum(II)" *Inorg. Synth.* **1997**, *31*, 284-286; (b) Clark, H. C.; Manzer, L. E., "Reactions of (π -1,5-cyclooctadiene)organoplatinum(II) compounds and the synthesis of perfluoroalkylplatinum complexes" *J. Organomet. Chem.* **1973**, *59*, 411-428.
24. Peters, R. G.; White, S.; Roddick, D. M., "Activation of Aromatic C-H Bonds by (dmpe)Pt(Me)X (X = Me, O₂CCF₃, OTf) Systems" *Organometallics* **1998**, *17*, 4493-4499.
25. Alexander, R. P.; Schroeder, H., "Chemistry of decaborane-phosphorus compounds. IV. Monomeric, oligomeric, and cyclic phosphinocarboranes" *Inorg. Chem.* **1963**, *2*, 1107-1110.
26. Kumada, M.; Sumitani, K.; Kiso, Y.; Tamao, K., "Silicon hydrides and nickel complexes. III. Hydrosilylation of olefins with dichloro[1,2-bis(dimethylphosphino)-1,2-dicarbido-closo-dodecaborane]nickel(II) as catalyst" *J. Organomet. Chem.* **1973**, *50*, 319-326.
27. Reed, C. A.; Fackler, N. L. P.; Kim, K.-C.; Stasko, D.; Evans, D. R.; Boyd, P. D. W.; Rickard, C. E. F., "Isolation of Protonated Arenes (Wheland Intermediates) with BARF and Carborane Anions. A Novel Crystalline Superacid" *J. Am. Chem. Soc.* **1999**, *121*, 6314-6315.
28. Olah, G. A.; Svoboda, J. J.; Olah, J. A., "Preparative carbocation chemistry. IV. Improved preparation of triphenylcarbenium (trityl) salts" *Synthesis* **1972**, 544.
29. Frisch, M. J. T., G. W.; Schlegel, H. B.; Scuseria, G. E.; Robb, M. A.; Cheeseman, J. R.; Scalmani, G.; Barone, V.; Mennucci, B.; Petersson, G. A.; Nakatsuji, H.; Caricato, M.; Li, X.; Hratchian, H. P.; Izmaylov, A. F.; Bloino, J.; Zheng, G.; Sonnenberg, J. L.; Hada, M.; Ehara, M.; Toyota, K.; Fukuda, R.; Hasegawa, J.; Ishida, M.; Nakajima, T.; Honda, Y.; Kitao, O.; Nakai, H.; Vreven, T.; Montgomery, Jr., J. A.; Peralta, J. E.; Ogliaro, F.; Bearpark, M.; Heyd, J. J.;

- Brothers, E.; Kudin, K. N.; Staroverov, V. N.; Kobayashi, R.; Normand, J.; Raghavachari, K.; Rendell, A.; Burant, J. C.; Iyengar, S. S.; Tomasi, J.; Cossi, M.; Rega, N.; Millam, N. J.; Klene, M.; Knox, J. E.; Cross, J. B.; Bakken, V.; Adamo, C.; Jaramillo, J.; Gomperts, R.; Stratmann, R. E.; Yazyev, O.; Austin, A. J.; Cammi, R.; Pomelli, C.; Ochterski, J. W.; Martin, R. L.; Morokuma, K.; Zakrzewski, V. G.; Voth, G. A.; Salvador, P.; Dannenberg, J. J.; Dapprich, S.; Daniels, A. D.; Farkas, Ö.; Foresman, J. B.; Ortiz, J. V.; Cioslowski, J.; Fox, D. J. Gaussian, Inc., Wallingford CT, 2009.
30. Zhao, Y.; Truhlar, D. G., "A new local density functional for main-group thermochemistry, transition metal bonding, thermochemical kinetics, and noncovalent interactions" *J. Chem. Phys.* **2006**, *125*, 194101.
31. Weigend, F.; Ahlrichs, R., "Balanced basis sets of split valence, triple zeta valence and quadruple zeta valence quality for H to Rn: Design and assessment of accuracy" *Phys. Chem. Chem. Phys.* **2005**, *7*, 3297-3305.
32. Andrae, D.; Haeussermann, U.; Dolg, M.; Stoll, H.; Preuss, H., "Energy-adjusted ab initio pseudopotentials for the second and third row transition elements" *Theor. Chim. Acta* **1990**, *77*, 123-141.

Suman Debnath: Investigation, Visualization, Validation. **Sayanti Basu:** Investigation, Visualization. **Bradley M. Schmidt:** Investigation. **Jeramie J. Adams:** Investigation, Visualization, Supervision. **Navamoney Arulsamy:** Investigation, Visualization. **Dean M. Roddick:** Conceptualization, Investigation, Visualization, Supervision, Methodology, Formal Analysis, Data Curation, Writing - Original Draft, Writing – Review & Editing, Project administration, Funding acquisition

Journal Pre-proofs

Kinetic and mechanistic studies for the previously reported $(dfep)Pt(Me)(NC_5F_5)^+$ ethylene dimerization catalyst system and a general extension to other chelating diphosphine analogues $(PP)Pt(Me)(C_2H_4)^+$ ($PP = dmpe, dippe, dppm, dppe, dppp, dppb, dmpe, dppc, dfppe$) are presented. Underlying factors for relative ethylene insertion barriers for diimine and diphosphine systems are evaluated.